University of Massachusetts
Transportation Center

Transportation Pooled Fund Study TPF-5(146):
Evaluation of Modified Performance Grade Binders in Thin Lift Maintenance Mixes and a Reflective Crack Relief Layer Mix

U.S. Department of Transportation
Federal Highway Administration

Moving Massachusetts Forward
massDOT
Massachusetts Department of Transportation

Deval L. Patrick
Governor

William F. Galvin
Acting Lieutenant Governor

Richard A. Davey
Secretary & CEO

December 2013 **Office of Transportation Planning** SPRII.06.26

This Page Left Intentionally Blank

Technical Report Document Page

1. Report No.	2. Government Accession No.	3. Recipient's Catalog No.
	N/A	N/A

4. Title and Subtitle	5. Report Date
Evaluation of Modified Performance Grade Binders in Thin Lift Maintenance Mixes and a Reflective Crack Relief Layer Mix	December 2013
	6. Performing Organization Code N/A

7. Author(s)	8. Performing Organization Report No.
Dr. Walaa S. Mogawer, P.E., F.ASCE Mr. Alexander J. Austerman, P.E.	UMTC-XX

9. Performing Organization Name and Address	10. Work Unit No. (TRAIS)
University of Massachusetts Dartmouth Highway Sustainability Research Center (HSRC) 151 Martine Street - Room 131, Fall River, MA 02723	N/A
	11. Contract or Grant No. ISA #

12. Sponsoring Agency Name and Address	13. Type of Report and Period Covered
Massachusetts Department of Transportation Office of Transportation Planning 10 Park Plaza, Suite 4150 Boston, MA 02116	Final
	14. Sponsoring Agency Code N/A

15. Supplementary Notes
N/A

16. Abstract

A polymer modified binder is required in a high performance thin asphalt overlay mixture because it has the ability of making the thin lift more elastic under traffic and less sensitive to temperature fluctuations. These thin mixtures typically have a thickness of one inch or less and are used in applications requiring higher levels of rutting and fatigue resistance.

A total of six asphalt binders were evaluated in this study. The binders were selected by a panel of members from the state agencies participating in the study. The binders were a PG64-28 with no modification, a PG64-28 with Polyphosphoric Acid (PPA) modification, a PG64-34 modified with Styrene Butadiene Styrene (SBS), a PG76-22 modified with SBS, a PG64-22 modified with 12% Ground Tire Rubber (GTR) and a PG64-28 modified with 2.0% latex. A Superpave 9.5mm mixture was designed using each of the six binders for this study and two sources of aggregates (crushed stone and gravel).

For the majority of the binder and mixture tests, the data showed that the modified binders performed better than the non-modified binders in terms of elastic recovery and mixture performance. The majority of the analyses identified the PG64-34 SBS as the most elastic binder and most fatigue resistance mixture. Furthermore, each binder was tested to determine its low temperature cracking resistance using the Asphalt Binder Cracking Device (ABCD). Each mixture was then tested for low temperature cracking resistance using the Asphalt Concrete Cracking Device (ACCD). Mastics corresponding to each mixture were tested for low temperature cracking resistance using the ABCD. Analysis of the results showed that the AASHTO critical cracking temperature had a strong correlation with the ABCD binder and mastics results, but did not correlate well with the mixture tests. Mastic testing generally did not correlate well with the mixture test results.

17. Key Word	18. Distribution Statement
Polymer Modified Binder, Ground Tire Rubber, Pavement Preservation, Thin Lift, Sustainable	No restrictions. This document is available to the public through the sponsoring agent.

19. Security Classif. (of this report)	20. Security Classif. (of this page)	21. No. of Pages	22. Price
Unclassified	Unclassified	46	N/A

Form DOT F 1700.7 (8-72) Reproduction of completed page authorized

This Page Left Intentionally Blank

Evaluation of Modified Performance Grade Binders in Thin Lift Maintenance Mixes and a Reflective Crack Relief Layer Mix

Final Report

Prepared By:

Dr. Walaa S. Mogawer, P.E., F.ASCE
Principal Investigator

Alexander J. Austerman, P.E.
Research Engineer

University of Massachusetts Dartmouth
Highway Sustainability Research Center
151 Martine Street – Room 131
Fall River, MA 02723

Prepared For:

Massachusetts Department of Transportation
Office of Transportation Planning
10 Park Plaza, Suite 4150
Boston, MA 02116

December 2013

This Page Left Intentionally Blank

Acknowledgements

Prepared in cooperation with the Massachusetts Department of Transportation Office of Transportation Planning, and the United States Department of Transportation Federal Highway Administration.

The research presented here was funded through the Transportation Pooled Fund Study TPF-5(146) funded by the transportation agencies of the participating states of Massachusetts (lead state), Rhode Island, New York, New Jersey, New Hampshire, and Connecticut. Specifically, the authors would like to thank the following pooled fund committee members for their input and assistance with the study: Ed Naras (MassDOT), Gary Frederick (NYSDOT), Gregory Doyle (FHWA Massachusetts Division Office), Clement Fung (MassDOT), Zoeb Zavery (NYSDOT), Colin Franco (RIDOT), Ed Kondrath (NJDOT), Allen Rawson (NHDOT) and Nelio Rodrigues (ConnDOT).

Finally the authors would like to acknowledge Aggregate Industries, Hudson Liquid Asphalt, SemMaterials, Citgo, Gorman Brothers, NuStar, and BASF for providing materials for this study.

Disclaimer

The contents of this report reflect the views of the authors, who are responsible for the facts and the accuracy of the data presented herein. The contents do not necessarily reflect the official view or policies of the Massachusetts Department of Transportation or the Federal Highway Administration. This report does not constitute a standard, specification, or regulation.

This Page Left Intentionally Blank

Table of Contents

List of Figures

List of Tables

Chapter One: Background

1.0 Introduction

Pavement experts have long believed that a superior hot-mix asphalt (HMA) used in thin lifts can be prepared by using a high performance elastic binder. This type of HMA is essential for rehabilitation and maintenance purposes throughout the northeast United States. A mixture with a high performance elastic binder can also be used in new pavement construction, like Open Graded Friction Course (OGFC) and Stone Matrix Asphalt (SMA).

High Performance Thin Asphalt Overlays (HPThinOL) incorporating a high performance elastic binder are defined as having a thickness of one inch or less and are used in applications requiring higher levels of rutting and fatigue resistance. Generally, HPThinOL are used as a pavement preservation strategy and are placed on pavements that have remaining structural capacity to last the expected life of the pavement preservation strategy. HPThinOL can seal pavements, reduce the rate of pavement deterioration, correct surface deficiencies, reduce permeability, correct rutting, and improve ride quality. Several Department of Transportation (DOT) agencies such as Arizona, Maryland, Michigan, New Jersey, New York, and Ohio have developed specifications for HPThinOL. These mixes are reported to be rut and crack resistance and to maintain excellent skid resistance. The specifications normally require the use of a high performance elastic binder known as a Polymer Modified Asphalt (PMA) binder. A PMA binder is required because it has the ability of making the HPThinOL more elastic under traffic and less sensitive to temperature fluctuations.

In this research project, HMA mixture designs with nominal maximum aggregates sizes (NMAS) of 9.5 mm were designed and evaluated using multiple PMA binders. These developed mixtures are the type that could be used for maintenance and rehabilitation. The mixtures were developed in order to address cracking (fatigue and low temperature) that commonly occur in flexible pavements in the Northeast.

Fatigue cracking occurring in HMA layers is one of the major distresses that occur in flexible pavements. It is function of load, thermal cycling over extended periods of time, material characteristics or a combination of these factors. Many state DOT agencies have required the use of PMA binders when fatigue cracking is an issue. Using the Superpave Performance Grade (PG) specification and tests for asphalt binders, the fatigue characteristic of the binder is commonly addressed by measuring the parameter $G^*\sin\delta$ at intermediate temperatures after long-term aging. This parameter was mainly developed for neat or non-modified asphalt binders. Because of this fact, additional binder testing is needed to address the fatigue characteristics of modified binders. In this study, the percent elastic recovery of asphalt binders was evaluated to determine if it can be used to address fatigue characteristics of HMA mixtures. The percent elastic recovery is measured using two simple binder tests: elastic recovery and Multiple Stress Creep Recovery (MSCR) Test. Elastic recovery is conducted using the ductility device following American Association of State Highway and Transportation Officials (AASHTO) T301 "Elastic Recovery Test of Asphalt Materials by Means of a Ductilometer" (*1*) and American Society for Testing and Materials (ASTM) D6084 Method A "Standard Test Method for Elastic Recovery of Bituminous Materials by Ductilometer"(*2*). The MSCR test is conducted using the Dynamic Shear Rheometer (DSR) following AASHTO TP70 "Multiple Stress Creep Recovery (MSCR) Test of Asphalt Binder Using a Dynamic Shear Rheometer (DSR)" (*3*) and ASTM D7405 "Standard Test Method for Multiple Stress Creep and Recovery (MSCR) of Asphalt Binder Using a Dynamic Shear Rheometer" (*2*). This test was developed by the Federal Highway Administration (FHWA) (*4,5,6*). It is hypothesized that the higher degree of elastic recovery or percent recovery in the MSCR test indicates a binder less prone to fatigue cracking in the HMA mixture. A high percent elastic recovery means that the binder, at a

certain stress level, will recover some percentage of the initial deformation. The high percent recovery should indicate a more elastic binder thereby leading to a HMA mixture with a relatively lower stiffness. A mixture with lower stiffness should be less prone to cracking. This hypothesis will be tested in this study by comparing the ranking of binder elasticity to the ranking of the mixture fatigue cracking characteristics measured using fracture mechanics and linear viscoelastic continuum damage approaches.

Three recently developed simple approaches were utilized to predict and evaluate the fatigue cracking of HMA mixtures. The first approach utilized the theory of fracture mechanics while the remaining two approaches were based on linear viscoelastic continuum damage theory. All of these analysis approaches are based on mechanistic more than empirical principles. These methods can provide HMA designers with more accurate models based on relationships between materials characteristics (chemical or mechanical) that are not attainable through empirical methods. These models can then be used for designing HMA mixtures that are more fatigue resistant. The fracture mechanics approach utilized was based on work by Zhou et al. (*7,8,9*) and has been validated using data from field test sites tested by the FHWA Accelerated Loading Facility (ALF) under Transportation Pooled Fund study TPF-5(019). This approach used a simple test, the Texas Overlay Test, coupled with the use of the mixture master curve data that is used as part of the new Mechanistic-Empirical Pavement Design Guide (MEPDG) Level 1 analysis. The Viscoelastic Continuum Damage (VECD) approach was based on work done by Kutay (*10*) and Christensen (*11,12*). Their work is a simplified model of work done initially by Schapery (*13*) and then used successfully by Kim (*14,15,16*). These approaches use a cyclic push-pull (tension-compression) test and the data from the mixture master curve. The cyclic push-pull test and the dynamic modulus test are both conducted using the same device, the Asphalt Mixture Performance Tester (AMPT). The results from the three mixture analysis approaches were compared and ranked in terms of fatigue cracking susceptibility. These mixture rankings were then compared to the rankings obtained from the binder elasticity testing. The comparison could indicate whether or not the binder elasticity tests can describe the fatigue cracking behavior of the mixture.

Another major distress that can occur in HMA layers is low temperature cracking. Low temperature cracking is a non-load associated distress which manifests itself in the form of transverse cracks that are typically evenly spaced along the pavement. Low-temperature cracking is a result of increased thermal stresses exceeding the tensile strength capacity of a HMA layer. This phenomenon occurs because as the ambient air temperature drops the HMA mixture becomes more stiff and brittle while concurrently contracting due to the temperature drop. The processes of contracting will induce thermal stresses in the HMA because the friction between the HMA layer and the underlying pavement structure will not permit the mixture from fully contracting (*17,18,19*). It is generally recognized by the HMA industry that the low temperature cracking performance of HMA mixtures are highly influenced by the properties of the asphalt binder utilized (*20*). The asphalt binder is the material governing the tensile strength of the mixture. In addition to the binder, it has been reported that low temperature cracking potential of HMA mixtures for a particular environment can be a function of binder content, aggregate type, aggregate gradation, and binder additives (ex. polymers or rubber).

Currently the low temperature cracking characteristics of an asphalt binder are characterized by ensuring the binder meets the low temperature parameters outlined in Table 1 of the Association of American State Highway and Transportation Officials (AASHTO) specification M320 “Performance-Graded Asphalt Binder” (*1*). However, AASHTO M320 Table 1 does not always properly characterize the low temperature properties of certain types of binders including physically and chemically modified binders (*21,22*). For this reason, AASHTO recently added an alternative binder specification to AASHTO M320, which is Table 2. In AASHTO M320 Table 2 the low temperature properties of the binder are characterized using a combination of Bending Beam Rheometer (BBR) and Direct Tension (DT) tests. A direct measurement of the low temperature cracking temperature of a binder is not possible via this method. The BBR test is utilized to determine the binders’ stiffness and the rate of change of the stiffness

(m-value) which is then used to calculate the thermal stress in a binder as the temperature drops. The DT is used to determine the low temperature tensile strength of the binder. The BBR and DT data are then used to calculate the critical cracking temperature (T_{cr}). This temperature is where the induced thermal stress on the binder equals the tensile strength of the binder. The determination of the binder critical cracking temperature requires a large number of test replicates and is based on lengthy analytical procedure that estimates thermal stress development using several assumptions (*23*). These assumptions include an estimate of the thermal expansion coefficient of binder and also time-temperature shift functions.

For characterizing the low temperature cracking performance of HMA mixtures, two approaches are currently being utilized. The first approach uses a mechanistic-empirical analysis and a performance model using tensile creep and strength data collected by performing AASHTO T322 "Determining the Creep Compliance and Strength of Hot-Mix Asphalt Using the Indirect Tensile Test Device"(*1*). This test is more commonly referred to as the indirect tensile test or IDT for short. The second mixture approach is a torture test known as the Thermal Stress Restrained Specimen Test (TSRST). This test is performed by cooling either a relatively long rectangular or circular beam specimen that has been glued to two metal platens. The specimen is cooled at a specified rate while it is restrained from contracting. As the beam cools, thermally induced tensile stresses develop as a result of it being restrained. When the induced tensile stress exceeds the tensile strength of the mixture, specimen failure occurs (*23,24*) and the failure temperature is recorded. This test provides a temperature at cracking like the AASHTO critical cracking temperature determination for binders. Although both of the mixture low temperature cracking tests have been validated with field performance and predict low-temperature cracking potential of HMA mixtures to a reasonable degree, it is believed that both methods have drawbacks. The IDT is a complex test and the analysis is also complex. Furthermore, studies have demonstrated that while the IDT may be a useful tool for estimating the low-temperature cracking performance of HMA, its predictions are based on assumptions including the mechanism of failure in the field, the thermal expansion coefficient of the mixture, and the assumption that behavior at the IDT testing temperatures can be used to adequately describe behavior at lower temperatures. The validity of these assumptions determines the accuracy of the predictions (*25,26,27,28*). Unlike the IDT, the TSRST is simple to conduct and the data analysis is simple and intuitive. However, sample preparation can be demanding because poor alignment may cause undesirable bending stresses, therefore leading to inaccurate fracture temperatures. Breaks immediately adjacent to one of the glued ends are also quite common because of the constraint provided by the glue (*25,26*).

Recently a different set of simple performance tests for measuring low temperature cracking resistance of asphalt binders (Asphalt Binder Cracking Device [ABCD]) and asphalt mixtures (Asphalt Concrete Cracking Device [ACCD]) have been developed and validated (*19,21,22*). Unlike the other low temperature cracking tests currently available, the ABCD and ACCD tests are much simpler to perform, make minimal assumptions, and repeatable. Both tests rely on measuring the cracking temperature while restraining the binder or mixture from contracting. In the study presented herein, the ABCD was used to measure the low-temperature cracking resistance of both binders and mixture mastics. The ACCD was used to measure the low-temperature cracking resistance of mixtures prepared using the same binders and two types of aggregates; crushed stone and gravel. The test results from the ABCD were compared to the results of current AASHTO M320 Table 2 tests for measuring the low temperature cracking of asphalt binders in an effort to determine if there is an agreement between the two methodologies. The binder and mastic results were compared to the ACCD results to determine which binder test has better agreement with the mixture test.

2.0 Objectives

The primary objective of this research project is to design and evaluate thin lift maintenance and rehabilitation HMA mixtures utilizing modified binders. For this project, thin lift mixes are defined as mixes that are placed at thicknesses greater than 3/4"and less than or equal to 1-1/2".

Specifically thin lift mixes with a NMAS of 9.5 mm will be developed using selected modified binders as maintenance and rehabilitation mixes using Superpave design methodology. The elasticity of the binders will be measured and evaluated as a tool to evaluate the resistance of the mixtures to fatigue cracking using fracture mechanics and viscoelastic damage theory. Furthermore, the mixes will then be evaluated for their resistance to low temperature cracking.

Chapter Two: Experimental Plan

1.0 Research Approach

Figures 1 illustrates the testing plan to evaluate if binder elasticity can be used as a simple performance test for fatigue cracking of polymer modified HMA mixtures. The objective of this part of the study, as stated previously, was to evaluate the elasticity of various binder grades (non-modified and modified) using the elastic recovery and MSCR tests, to study the effect of various binder grades (non-modified and modified) on the fatigue characteristics of HMA mixture using fracture mechanics and viscoelastic continuum damage approaches, to evaluate the relationship between the elastic recovery of the asphalt binder and the fatigue resistance of the HMA mixture, and to compare the rankings of the mixture fatigue characteristics obtained by the fracture mechanics and viscoelastic continuum damage approaches to determine if the rankings provided are similar.

Figure 2 illustrates the testing plan to evaluate the effect of binder type, mastic, and aggregate type on the low temperature characteristics of modified hot mix asphalt. The objectives of this part of the study was: to measure the continuous low temperature grade and critical cracking temperature (T_{cr}) of different binders using current AASHTO M320 procedures, to measure the low cracking temperature of unaged and aged (RTFO and PAV) binder samples using AASHTO TP 92-11 'Determining the Cracking Temperatures of Asphalt Binder Using the Asphalt Binder Cracking Device (ABCD)', to measure the low temperature cracking performance of asphalt mixtures using the ACCD. The mixtures were fabricated using six different binders and two sources of aggregates, to measure the low cracking temperatures of each mixture's mastic using the ABCD, to compare and correlate the following eight sets of data: (1) continuous low temperature grades of the binders, (2) critical cracking temperature (T_{cr}) of the binders, (3) ABCD cracking temperatures using unaged binders, (4) ABCD cracking temperatures using aged binders, (5) ABCD cracking temperatures using mastics fabricated from crushed stone material, (6) ABCD cracking temperatures using mastics fabricated from gravel material, (7) ACCD cracking temperatures using mixtures fabricated from the crushed stone, and (8) ACCD cracking temperatures using mixtures fabricated from the gravel, to evaluate the significance of aging a binder when using the ABCD, to determine the influence of binder type and aggregate type on low temperature cracking characteristics of asphalt mixtures, and to determine the effect of aggregate type on both mastic and mixture performance.

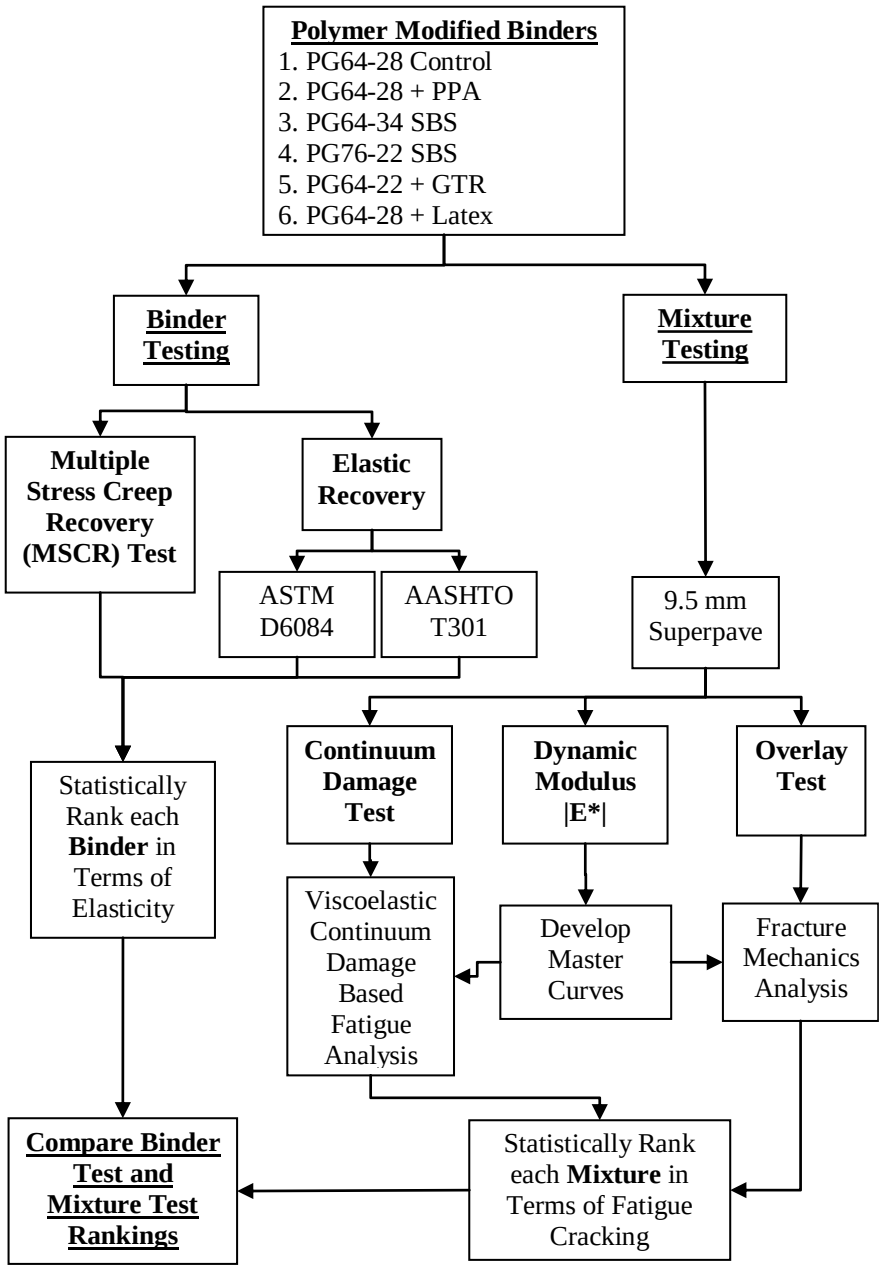

Figure 1. Testing Plan to Measure Binder Elasticity and Mixtures Fatigue Characteristics

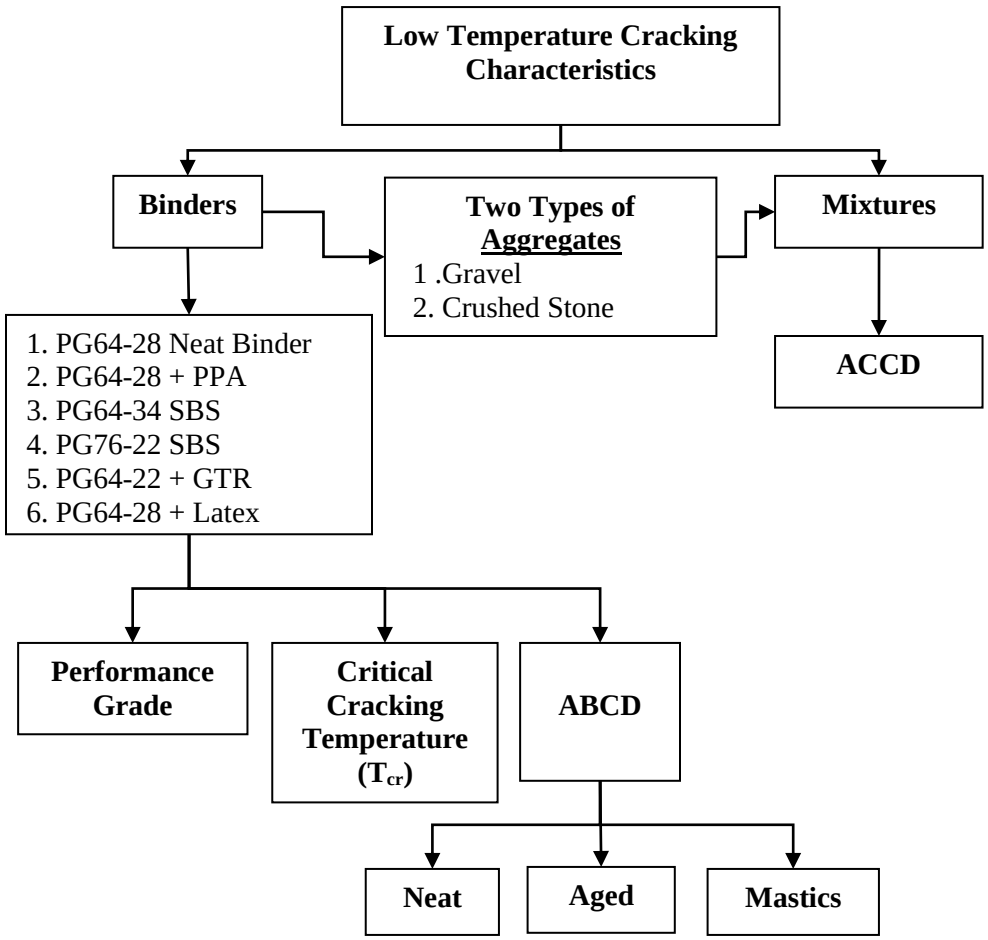

Figure 2. Testing Plan to Measure Effect of Binder Modification on Low Temperature Characteristics of Binders, Mastics, and Mixtures.

2.0 Materials

The following sections outline properties of the material utilized for this study.

2.1 Binder

For this study, a total of six different asphalt binders were utilized. The binders were selected by a panel of members with expertise in asphalt materials. These members were from the state agencies participating in the pooled fund study. The binder selection was based on each member's interest in utilizing a particular binder for future projects or prior successful utilization in past projects. The selected non-modified and modified binders that were utilized in this study are shown in Table 1. Additionally, this table indicates the source of the binder and the type of modification utilized, if any. Table 2 shows the mixing and compaction temperatures utilized for each binder throughout the study.

Table 1. Performance Grade, Source, Type of Modifications and Average Properties of Binders

	PG64-28 Control Neat Binder	PG64-28 + PPA	PG64-34 SBS	PG76-22 SBS	PG64-22 + GTR	PG64-28 + Latex
Source	Aggregate Industries	Hudson Asphalt	Sem Materials	Citgo Asphalt	Gorman	Base PG64-28 Aggregate Industries
Modification	None	Poly Phosphoric Acid (PPA)	Styrene-Butadiene -Styrene (SBS)	Styrene-Butadiene -Styrene (SBS)	12% Ground Tire Rubber (GTR)	2.0% Latex (BASF Butanol NX1129)
PG Grade	PG64-28	PG64-28	PG64-34	PG76-22	PG88-16	PG70-22
Continuous Grade	67.9-29.2	66.4-29.6	69.9-36.1	80.8-27.6	88.7-19.8	75.2-26.3
AASHTO T315 DSR G*/sinδ (kPa) – Original	1.551 @ 64ºC	1.321 @ 64ºC	1.542 @ 64ºC	1.546 @ 76ºC	1.055 @ 88ºC	1.664 @ 70ºC
AASHTO T315 DSR G*/sinδ (kPa) – RTFO Residue	4.424 @ 64ºC	3.646 @ 64ºC	3.209 @ 70ºC	3.614 @ 76ºC	3.949 @ 88ºC	2.774 @ 76ºC
AASHTO T315 DSR G* sinδ (kPa) – PAV Residue	4,891 @ 19ºC	3,593 @ 19ºC	1,870 @ 19ºC	1,791 @ 28ºC	808 @ 34ºC	1,020@ 25ºC
AASHTO T313 BBR Creep Stiffness @ 60s S(MPa)	263 @ -18ºC	192 @ -18ºC	216 @ -24ºC	144 @ -12ºC	43.6 @ -6ºC	145 @ -12ºC
AASHTO T313 BBR Slope @ 60s m-value	0.316 @ -18ºC	0.315 @ -18ºC	0.322 @ -24ºC	0.350 @ -12ºC	0.318 @ -6ºC	0.330 @ -12C

Table 2. Binder Mixing and Compaction Temperatures

Binder	Mixing Temperature Range	Compaction Temperature Range
PG64-28 Control	165-161ºC [1]	157-153ºC [1]
PG64-28 + PPA	163-159ºC [1]	154-149ºC [1]
PG64-34 SBS	154-150ºC [2]	143-139ºC [2]
PG76-22 SBS	163-157ºC [2]	157-152ºC [2]
PG64-22 + GTR	171-158ºC [2]	146-135ºC [2]
PG64-28 + Latex	172 ºC [3]	169 ºC [3]

[1] Temperatures based on binder viscosity measurements (AASHTO T316) as outlined in AASHTO T312.
[2] Recommended temperatures supplied by asphalt manufacturer.
[3] Temperatures based on recommendation of latex supplier.

2.2 Aggregates

Two different types of aggregates were utilized for this project, crushed stone and gravel. The crushed stone originated from a source in Wrentham, Massachusetts, whereas the gravel originated from a source in Farmington, NH. The aggregate properties of each stockpile are shown in Table 3. Two types of aggregates were included in the study to measure the effect of aggregate type on the low temperature characteristics of HMA mixtures. The coarse portion of the gravel was less angular and had higher absorption than the crushed stone.

Table 3. Average Aggregate Stockpile Properties

	Crushed Stone Source			**Gravel Source**			
Sieve Size	**9.5 mm Crushed Stone**	**Stone Dust**	**Washed Sand**	**9.5mm Gravel**	**Dust**	**Grits**	**Washed Sand**
19.0 mm	100	100	100	100.0	100.0	100.0	100.0
12.5 mm	99.9	100	100	100.0	100.0	100.0	100.0
9.5 mm	96.7	100	100	100.0	100.0	100.0	100.0
4.75 mm	37.5	99.4	98.6	38.1	98.6	100.0	100.0
2.36 mm	3.3	81.6	81.7	7.0	75.5	84.5	91.3
1.18 mm	1.7	56.1	56.5	3.0	56.9	60.3	72.2
0.600 mm	1.6	38.4	38.1	1.8	43.6	39.5	45.6
0.300 mm	1.6	25.3	23.5	1.3	31.7	19.9	19.3
0.150 mm	1.5	16.1	12.7	0.9	19.8	6.4	4.7
0.075 mm	1.4	11.2	6.6	0.6	11.9	2.7	2.0
Mix Design Proportions, %	49.8	25.1	25.1	51.4	28.0	12.7	7.9
Specific Gravity, Gsb (AASHTO T84/T85)	2.611	2.600	2.631	2.622	2.659	2.608	2.628
Absorption, %	0.54%	0.77%	0.51%	0.86%	0.48%	1.01%	0.75%
Coarse Aggregate Angularity, % (ASTM D4791)	97.0%	n/a	n/a	92.0%	n/a	n/a	n/a
Flat and Elongated Particles, % (ASTM D5821)	3.0%	n/a	n/a	2.0%	n/a	n/a	n/a
Fine Aggregate Angularity, % (AASHTO T304)	n/a	47.2	47.9	n/a	50.7	48.0	44.0
Sand Equivalent, % (AASHTO T176)	n/a	73	90	n/a	80	98	97.0

2.3 Mastics

Mastics were prepared for each of the six different binders and the two aggregate types included in this study. Mastics were prepared by mixing the minus No. 200 material from the appropriate aggregate type with each of the binders. The ratio needed to fabricate mastic specimens was determined from the ratio of minus No. 200 material to effective binder content for each corresponding HMA mixture. These ratios are shown in Table 4.

Table 4. Ratio of Minus No. 200 Material to Effective Binder Content of the Mixture Utilized for Mastic Preparation

Binder	Crushed Stone Source	Gravel Source
PG64-28 Neat Binder	0.77	0.62
PG64-28 + PPA	0.76	0.62
PG64-34 SBS	0.73	0.60
PG76-22 SBS	0.77	0.62
PG64-22 + GTR	0.59	0.48
PG64-28 + Latex	0.71	0.57

3.0 Mixture Design

A 9.5 mm Superpave mixture was developed for each aggregate type (crushed stone and gravel) in accordance with AASHTO M323 "Superpave Volumetric Mix Design" and AASHTO R35 "Superpave Volumetric Design for Hot Mix Asphalt" (*1*) using each of the six asphalt binders. The mixtures designs were coarse-graded Superpave 9.5mm. The design mixture gradation and combined aggregate properties for each design are shown in Table 5.

Table 5. Mixture Gradations and Combined Aggregate Properties

Sieve Size	Crushed Stone 9.5 mm Mixture Gradation	Gravel 9.5 mm Mixture Gradation	9.5 mm Superpave Specification Range
12.5 mm	100	100	100 min.
9.5 mm	98.4	100	90-100
4.75 mm	68.4	67.8	90 max.
2.36 mm	42.6	42.7	32-67
1.18 mm	29.1	30.8	-
0.600 mm	20.0	21.8	-
0.300 mm	13.0	13.6	-
0.150 mm	8.0	7.2	-
0.075 mm	5.2	4.1	2-10
Coarse Aggregate Angularity, % (ASTM D4791)	97.0%	92.0%	95/90
Flat and Elongated Particles, % (ASTM D5821)	3.0%	2.0%	10 max.
Fine Aggregate Angularity, % (AASHTO T304)	47.6%	48.9%	45% min.
Sand Equivalent, % (AASHTO T176)	86.5%	87.5%	45% min.
Combined Specific Gravity , G_{sb}	2.613	2.631	-

The design Equivalent Single Axle Loads (ESALs) for this project was selected to be 3 to <30 million. This ESALs level was consistent with high traffic surface course mixtures in New England. The design Superpave gyratory compactive effort for this ESALs level was N_{design} = 100 gyrations.

Specimens were batched, mixed and short-term aged at the compaction temperature for two hours in accordance with AASHTO R30 "Mixture Conditioning of Hot Mix Asphalt (HMA)" (*1*). After aging, specimens (150 mm diameter) were compacted in the Superpave Gyratory Compactor (SGC) to N_{design}. The volumetric properties of the SGC mix design specimens for each aggregate type and binder are shown in Table 6. Mixture were designed to meet the Superpave volumetric requirements for air voids, Voids in Mineral Aggregate (VMA), Voids Filled with Asphalt (VFA), and Dust to Binder Ratio. In some instances it was not possible to meet the VFA requirements since AASHTO M323 specifies an increase in the acceptable VFA range from 65-75% to 73-76% for 9.5 mm mixtures with design traffic levels greater than 3 million ESALs. In these cases the mixtures were designed as close to the VFA range as possible without negatively impacting the other volumetric properties.

Table 6. Superpave 9.5 mm Mixture Properties at N_{design}

Properties	**Crushed Stone PG64-28 Neat Binder**	**Crushed Stone PG64-28 + PPA**	**Crushed Stone PG64-34 SBS**	**Gravel PG64-28 Neat Binder**	**Gravel PG64-28 + PPA**	**Gravel PG64-34 SBS**	**Superpave Spec.**
Binder Content, %	5.80	5.80	5.80	6.10	6.10	6.10	-
Pbe[a], %	5.08	5.16	5.34	5.38	5.36	5.56	-
Air Voids,%	3.9	4.3	4.1	4.5	4.8	4.0	4.0%
VMA[b], %	15.5	15.9	16.2	16.7	16.9	16.6	15% min.
VFA[c], %	74.6	73.3	74.6	73.0	71.4	76.1	73 – 76
Dust to Binder Ratio	0.8	0.8	0.8	0.65	0.65	0.60	0.6 -1.2
Properties	**Crushed Stone PG76-22 SBS**	**Crushed Stone PG64-22 + GTR**	**Crushed Stone PG64-28 + Latex**	**Gravel PG76-22 SBS**	**Gravel PG64-22 + GTR**	**Gravel PG64-28 + Latex**	**Superpave Spec.**
Binder Content, %	5.80	7.30	6.25	6.10	7.60	6.50	-
Pbe[a], %	5.10	6.50	5.53	5.36	6.78	5.80	-
Air Voids,%	3.5	4.0	4.5	4.4	3.7	4.1	4.0%
VMA[b], %	15.1	18.5	16.9	16.5	18.9	17.3	15% min.
VFA[c], %	77.1	78.3	73.4	73.4	80.3	76.1	73 – 76
Dust to Binder Ratio	0.8	0.6	0.8	0.65	0.5	0.6	0.6 -1.2

[a]Pbe = Percent Binder Effective [b]VMA = Voids in Mineral Aggregate [c]VFA = Voids Filled with Asphalt

Chapter Three: Utilizing Linear Viscoelastic Continuum Damage and Fracture Mechanics Approaches to Evaluate Binder Elasticity as a Simple Performance Test for Fatigue Cracking of Polymer Modified HMA Mixtures

1.0 Elastic Recovery of Asphalt Binders Approach

1.1 Elastic Recovery Test

Elastic recovery testing of each binder was performed in accordance with AASHTO T301 " Elastic Recovery Test of Asphalt Materials by Means of a Ductilometer"(*1*) and ASTM D6084 Method A "Standard Test Method for Elastic Recovery of Bituminous Materials by Ductilometer" (*2*). Each of these test was performed on the aged residue of each binder after aging in the Rolling Thin Film Oven (RTFO) in accordance with AASHTO T240 "Effect of Heat and Air on a Moving Film of Asphalt (Rolling Thin-Film Oven Test)" (*1*). Additionally, AASHTO T301 was conducted on each binder in the un-aged (as received) condition for comparison purposes. All elastic recovery testing for this study was conducted at 25ºC per the ASTM specification.

In the elastic recovery test, the binder specimens are pulled part in a ductilometer and held after reaching a specified elongation. The specimens are then cut in the middle of the elongation and the percent recovery of each specimen determined. The main differences between the AASHTO T301 and ASTM D6084 Method A utilized in this study are summarized in Table 7. The results of the testing are shown in Tables 8 and 9.

Table 7. Comparison of Elastic Recovery Methods

Test Parameter	AASHTO T301	ASTM D6084 Method A
Elongation Speed	5 cm/minute	Uniform Speed
Total Elongation	20 cm	10 ± 0.25cm
Wait Time Until Specimen is Cut After Elongation	5 minutes	None
Hold Time Until Recovery Measurement	60 minutes	60 minutes

Table 8. Binder Test Results

	PG64-28 Control	PG64-28 + PPA	PG64-34 SBS
Binder Grading			
Performance Grade (PG)	PG64-28	PG64-28	PG64-34
Continuous Grade	67.9-29.2	66.4-29.6	69.9-36.1
Elastic Recovery			
Percent Recovery (AASHTO T301 Unaged)	0	4	93
Percent Recovery (AASHTO T301 RTFO Aged)	10	7	89
Percent Recovery (ASTM D6084 Method A RTFO Aged)	35	30	95
Multiple Stress Creep Recovery			
Percent Recovery -100 Pa	12.5	20.3	88.7
Percent Recovery -3,200 Pa	4.35	4.2	88.7
Percent Difference Between Average Recovery Values	65.2	79.2	0

Table 9. Binder Test Results (Continued)

	PG76-22 SBS	PG64-22 + GTR	PG64-28 + Latex
Binder Grading			
Performance Grade (PG)	PG76-22	PG88-16	PG70-22
Continuous Grade	80.8-27.6	88.7-19.8	75.2-26.3
Elastic Recovery			
Percent Recovery (AASHTO T301 Unaged)	63	BDE	69
Percent Recovery (AASHTO T301 RTFO Aged)	65	BDE	63
Percent Recovery (ASTM D6084 Method A RTFO Aged)	77.5	75	67.5
Multiple Stress Creep Recovery			
Percent Recovery -100 Pa	51.6	52.9	31.4
Percent Recovery -3,200 Pa	30.7	11.1	15.7
Percent Difference Between Average Recovery Values	40.7	79.1	50.0

BDE = Broke During Elongation

1.2 Multiple Stress Creep Recovery Test

The Multiple Stress Creep Recovery (MSCR) test was conducted for each binder included in this study in accordance with AASHTO TP70 "Multiple Stress Creep Recovery (MSCR) Test of Asphalt Binder Using a Dynamic Shear Rheometer (DSR)" (*3*) and ASTM D7405 "Standard Test Method for Multiple Stress Creep and Recovery (MSCR) of Asphalt Binder Using a Dynamic Shear Rheometer" (*2*). Specimens of each binder were tested after RTFO aging in accordance with AASHTO T240. Each specimen was

tested at the high Performance Grade (PG) temperature of the binder and the average percent recovery at creep stress levels of 100 Pa and 3,200 Pa was determined. The results for the MSCR test are shown in Tables 8 and 9.

1.3 Results and Analysis

Tables 8 and 9 show that the PG64-34 SBS exhibited the highest percent elastic recovery for both the unaged and RTFO aged binder when tested in accordance with AASHTO T301. Additionally, the PG64-34 SBS had the highest percent recovery at both stress levels in the MSCR test. Furthermore, the binder data indicated that the PG76-22 SBS and PG64-28 + latex did not perform as well in the elastic recovery and MSCR tests as the PG64-34 SBS but their performance was better than the PG64-28 + PPA, PG64-28 Control and PG64-22 + GTR. The PG64-22 + GTR broke before reaching the 20 cm elongation in the AASHTO T301 test elastic recovery test. However, this binder performed much better in the ASTM D6084 Method A elastic recovery procedure which required a specimen elongation of only 10 cm. Comparing the elastic recovery data for the PG64-22 + GTR, it appeared that the binder was sensitive to the strain level applied.

A statistical analysis was performed on the binder testing data in order to establish ranking of each binder it terms of elasticity. These rankings are shown in Tables 10 and 11. The letters are the rankings provided by Duncan's statistical procedure, which is performed in conjunction with an analysis of variance at a 0.05 significance level. The Duncan procedure determines which averages are not significantly different from other averages. Averages that are not significantly different have the same letter.

Table 10. Statistical Ranking of Binders Based on Binder Elasticity Testing

	Percent Recovery		
Binder	**AASHTO T301 Unaged**	**AASHTO T301 RTFO aged**	**ASTM D6084 Method A**
PG64-28 Control	E	D	E
PG64-28 + PPA	D	E	F
PG64-34 SBS	A	A	A
PG76-22 SBS	C	B	B
PG64-22 + GTR	No Test Data	No Test Data	C
PG64-28 + Latex	B	C	D

Note: Letters represent the statistical ranking with "A" denoting the test results providing the highest percent recovery.

Table 11. Statistical Ranking of Binders Based on Binder Testing

Binder	**MSCR Percent Recovery - 100 Pa**	**MSCR Percent Recovery - 3200 Pa**
PG64-28 Control	E	E
PG64-28 + PPA	D	F
PG64-34 SBS	A	A
PG76-22 SBS	B	B
PG64-22 + GTR	B	D
PG64-28 + Latex	C	C

Note: Letters represent the statistical ranking with "A" denoting the test results providing the highest percent recovery.

2.0 Dynamic Modulus Testing

Complex dynamic modulus |E*| testing was conducted to determine the impact of the binder type and modification on the overall mixture stiffness. Additionally this data was needed to perform the OT based fracture mechanics analysis and the Viscoelastic Continuum Damage analyses.

In order to determine the dynamic modulus, test specimens were subjected to a sinusoidal (haversine) axial compressive stress at the different temperatures and frequencies in the Asphalt Mixture Performance Test (AMPT) device. The resultant recoverable axial strain (peak-to-peak) was measured. From this data, the dynamic modulus was calculated. The dynamic modulus data was then utilized to develop mixture master curves. The master curve shows the stiffness of the mixture in terms of dynamic modulus over varying temperatures and frequencies.

10.1 Specimen Fabrication and Testing

The dynamic modulus test specimens were fabricated using the Superpave Gyratory Compactor (SGC). Similar to the mix design process, each mixture was batched, mixed and short-term aged at 135ºC for four hours in accordance with AASHTO R30 "Mixture Conditioning of Hot Mix Asphalt (HMA)." After aging, specimens (150 mm diameter x 170 mm tall) were compacted in the SGC. These specimens were subsequently cored and then cut to the final specimen dimensions of 100 mm in diameter by 150 mm tall as suggested in AASHTO TP62 "Determining Dynamic Modulus of Hot Mix Asphalt (HMA)"(*3*) and NCHRP Report 614 "Proposed Standard Practice for Preparation of Cylindrical Performance Test Specimens Using the Superpave Gyratory Compactor" (*29*). Each cut specimen was tested to determine the air voids. The target air void range was 7±1% which correlated to the expected in place density after construction. Three replicate dynamic modulus specimens were fabricated for each binder included in this study. Four additional specimens were fabricated to the same dimensions and air void target for the continuum damage testing outlined later in this chapter.

Dynamic modulus testing was completed in AMPT in accordance with AASHTO TP62 (*3*) and the draft specification provided in NCHRP Report 614 (*29*). Specimens for all binders except the PG76-22 SBS were tested at temperatures of 4°C, 20°C, and 40°C and loading frequencies of 10 Hz, 1 Hz, 0.1 Hz, and 0.01 Hz (40°C only) as suggested in the specification provided in NCHRP Report 614 "Proposed Standard Practice for Developing Dynamic Modulus Master Curves for Hot-Mix Asphalt Concrete Using the Simple Performance Test System" (*29*). An additional temperature of 50°C with loading frequencies of 10 Hz, 1 Hz, 0.1 Hz, and 0.01 Hz was added to the testing regime for these specimens for use in the continuum damage analysis presented later. The specimens fabricated with the PG76-22 SBS binder were tested at temperatures of 4°C, 20°C, and 45°C and loading frequencies of 10 Hz, 1 Hz, 0.1 Hz, and 0.01 Hz (45°C only) as suggested in the specification provided in NCHRP Report 614 (*29*). Similarly, an additional temperature of 55°C with loading frequencies of 10 Hz, 1 Hz, 0.1 Hz, and 0.01 Hz was added for use in the continuum damage analysis. This extra temperature allows computation of lower tail (i.e, low frequency high temperature) region of the |E*| master curve. This in turn leads to more accurate computation of E(t) master curve (through interconversion) and continuum damage parameter α.

The results of the dynamic modulus testing are shown in Figures 3 and 4. Error bars on these dynamic modulus charts indicate the confidence interval for the data. Error bars that do not overlap indicate a significant difference in the measured stiffness between the specimens.

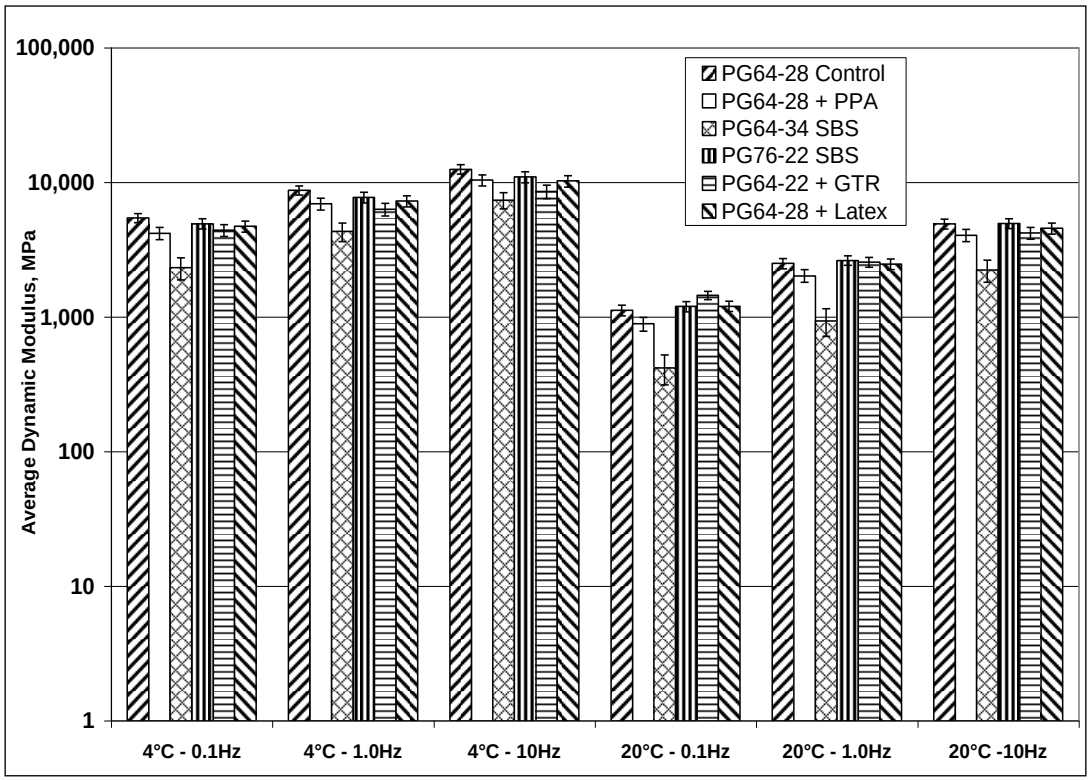

Figure 3. 9.5 mm Superpave Dynamic Modulus Comparison – Low and Intermediate Temperatures

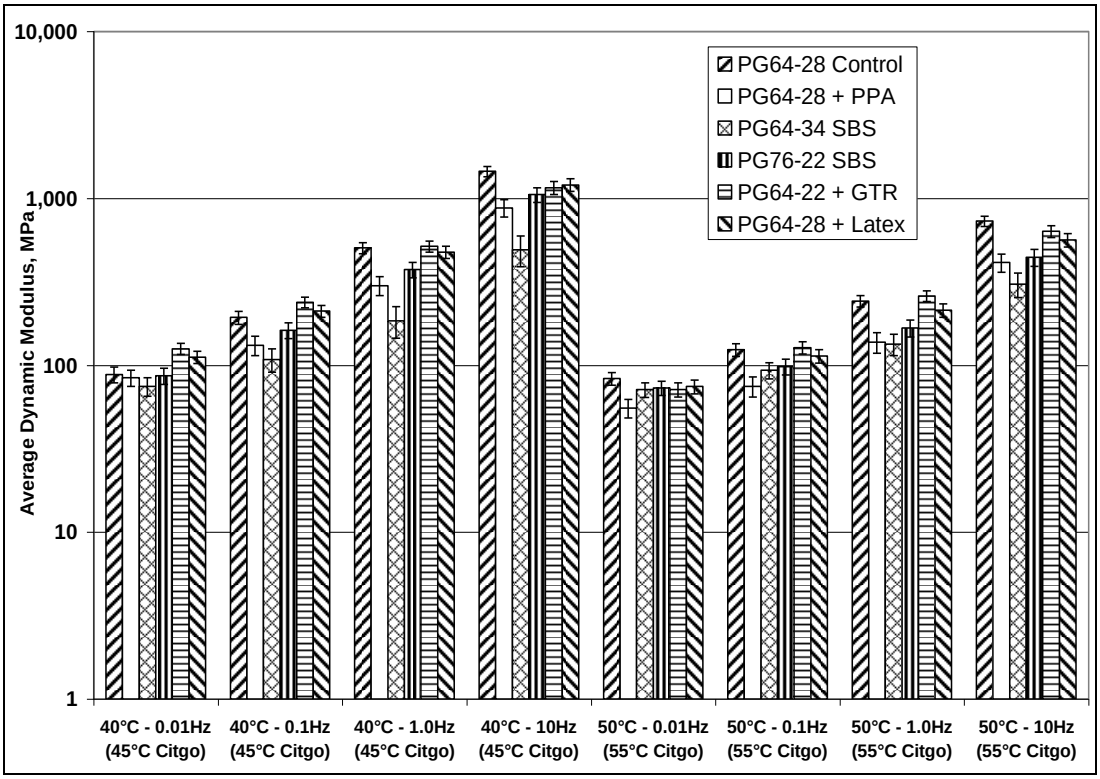

Figure 4. 9.5 mm Superpave Dynamic Modulus Comparison – High Temperatures

The dynamic modulus data was then utilized to develop mixture master curves for each binder type. Mixture master curves were developed using the specification provided in NCHRP Report 614 "Proposed Standard Practice for Developing Dynamic Modulus Master Curves for Hot-Mix Asphalt Concrete Using the Simple Performance Test System" (*29*). The master curves at a reference temperature of 15ºC (representative of intermediate temperatures in the northeast United States) for all mixtures tested are shown in Figure 5.

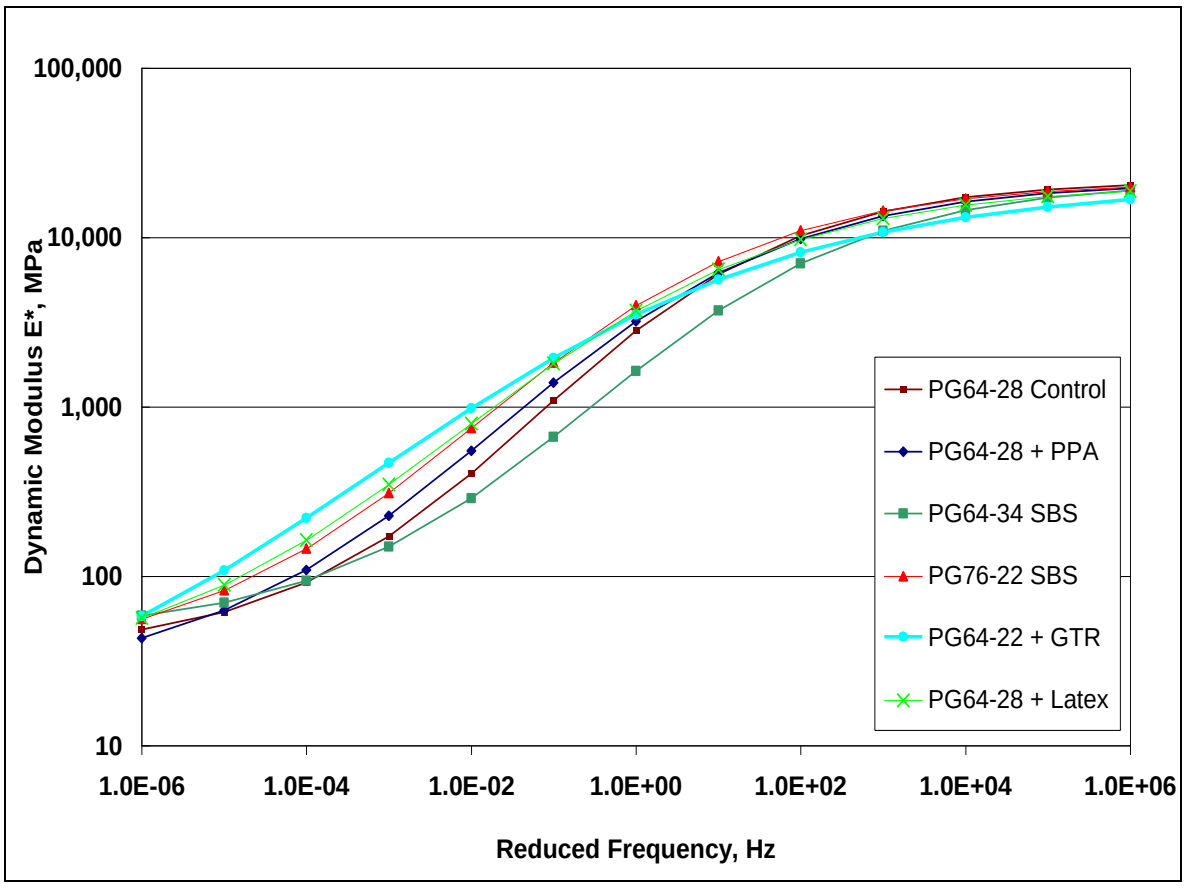

Figure 5. 9.5 mm Superpave Mixture Master Curves at Reference Temperature of 15ºC

3.0 Fracture Mechanics Approach

The Overlay Test (OT) based fracture mechanics approach developed by Zhou et al. (*7,8*) assumes that fatigue cracking is the combination of crack initiation and crack propagation process. Thus, both crack initiation and crack propagation are included in the fatigue analysis. Furthermore, the OT-based fracture mechanics approach for fatigue cracking prediction has three key components: fatigue life model, fatigue damage model, and fatigue area model.

The load repetitions (N_f) to cause a crack to initiate and propagate through asphalt surface layer is the sum of the number of load repetitions needed for micro-cracks to coalesce to initiate a macro-crack (crack initiation, N_i) and the number of load repetitions required for the macro-crack to propagate to the surface (crack propagation, N_p):

$$N_f = N_i + N_p \qquad \text{(EQN.1)}$$

Crack initiation life N_i is estimated using the following equations:

$$N_i = k_1\left(\frac{1}{\varepsilon}\right)^{k_2} \quad \text{(EQN. 2)}$$

$$k_1 = 10^{6.97001-3.20145k_2-0.83661\log E} \quad \text{(EQN. 3)}$$

$$k_2 = n \quad \text{(EQN. 4)}$$

where ε is maximum tensile strain at the bottom of asphalt layer; E is dynamic modulus; and n is fracture property. Crack propagation life N_p is calculated based on the well-known Paris' law:

$$N_p = \int_{c_0}^{h} \frac{1}{A(K)^n} dc \quad \text{(EQN. 5)}$$

In equation 5, c_0 is initial crack length (based on Lytton's recommendation [*30*], c_0=7.5 mm is used for later analysis); h is asphalt layer thickness; K is stress intensity factor calculated from finite element program such as CrackPro (*31*); and A and n are fracture properties determined from the OT testing.

The fatigue damage (D) caused by a specified number of load repetitions (n) is estimated using Miner's law:

$$D = \sum \frac{n}{N_f} \quad \text{(EQN. 6)}$$

A sigmoidal model is proposed for predicting fatigue area:

$$fatigue\_area(\%) = \frac{100}{1+e^{-7.89\log D}} \quad \text{(EQN .7)}$$

where D is fatigue damage estimated from Equation 6. Note that the fatigue cracking area is percentage of wheel path.

3.1 Specimen Fabrication and Testing

Reviewing above models, it is clear that both the dynamic modulus test and the OT are required for using the fracture mechanics approach. The dynamic modulus test has been described previously. OT specimens were fabricated in the SGC. Three specimens were fabricated for each binder type included in this study. Specimens were cut to the dimensions required for the OT as outlined in Texas Department of Transportation Specification Tex-248-F "Overlay Test" (*32*). The densities obtained for these OT specimens are shown in Table 12. Each specimen was conditioned for three hours at the testing temperature of 15ºC which is representative of intermediate temperatures in the northeast United States. Testing was conducted with a Maximum Opening Displacement (MOD) of 0.6 mm applied over a ten second interval. Test termination (failure) occurred when the maximum cyclic load dropped 93% from the initial maximum load measured at the first cycle. The typical setup for testing HMA in the OT is shown in Figure 6. The test results and the determined fracture properties for each mixture are shown in Table 12.

Figure 6. Typical Overlay Test Setup

Table 12. OT Specimens Density, Test Results, and Fracture Properties

Binder Type	Replicate No.	Actual Specimen Density, %	Cycles to Failure	*A*	*n*
PG64-28 Control	1	92.3	1111	4.42E-8	3.6969
	2	93.0	285	8.52E-8	3.6631
	3	93.2	345	5.76E-8	3.7274
	Average	92.8	580	6.23E-8	3.6958
PG64-28 + PPA	1	93.2	>1200	3.00E-8	4.0611
	2	93.2	>1200	2.91E-8	4.0629
	3	93.1	>1200	2.38E-8	4.1155
	Average	93.2	>1200	2.76E-8	4.0798
PG64-34 SBS	1	93.6	>1200	2.33E-8	4.9113
	2	94.2	>1200	1.54E-8	5.0342
	3	93.5	>1200	3.03E-8	4.8519
	Average	93.8	>1200	2.30E-8	4.9325
PG76-22 SBS	1	92.7	312	5.68E-8	3.6302
	2	93.9	1008	2.23E-8	3.7580
	3	93.1	687	3.77E-8	3.6399
	Average	93.2	669	3.89E-8	3.6760
PG64-22 + GTR	1	92.5	172	2.35E-7	3.7216
	2	92.4	85	5.73E-7	3.4779
	3	92.1	81	2.87E-7	3.7729
	Average	92.3	112	3.65E-7	3.6575
PG64-28 + Latex	1	92.6	470	4.24E-8	3.7083
	2	93.0	874	5.63E-8	3.7123
	3	92.5	165	7.80E-8	3.8080
	Average	92.7	503	5.89E-8	3.7429

3.2 Results

As noted previously, the mixtures were designed at a traffic level of 3 to less than 30 million ESALs over a 20 year design life. Similarly, in this study a very high traffic volume was assumed with 28 million

ESALs in 20 years and a 3% annual growth rate. Also, a weather station located in Boston, MA was used as the input to the Enhanced Integrated Climatic Model (EICM) to predict pavement temperatures for analyzing fatigue cracking development.

To compare fatigue performance of the control and modified binders used in this study, three basic pavement structures with 50 mm, 100 mm, and 150 mm thick asphalt layer shown in Figure 7 were assumed. For each pavement structure, all layers properties and thickness were constant except the asphalt layer. The asphalt layer varied due to the six different modified binders utilized for the mixture. A total of 18 pavement structures (1 mixture×6 binders ×3 asphalt layer thicknesses) were analyzed. For each specific pavement structure, asphalt layer monthly modulus was determined based on monthly pavement temperature from EICM, dynamic modulus master curve, and traffic vehicle speed (v=96 km/h). The final fatigue cracking area developments for these pavement structures are presented in Figures 8, 9, and 10.

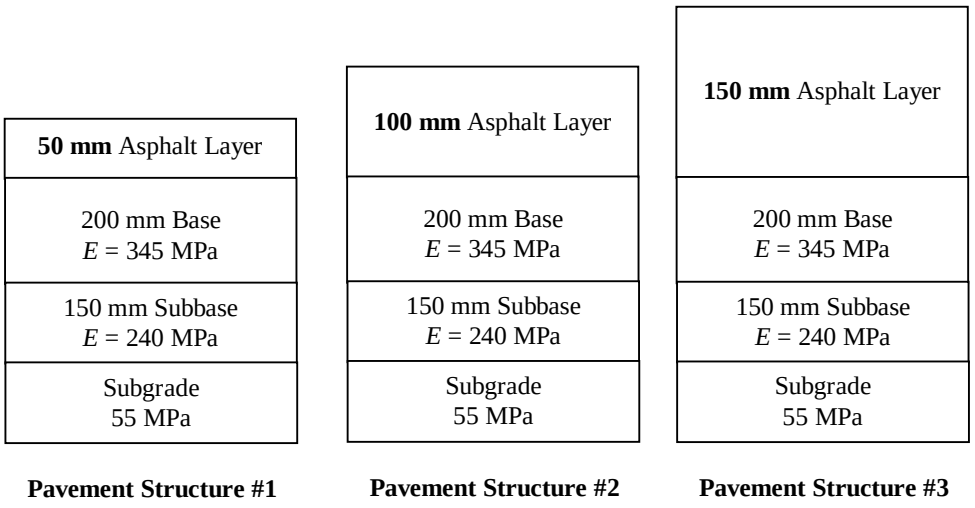

Figure 7. Three Basic Pavement Structures Used for Fatigue Analysis

Reviewing the fatigue analysis results presented in Figures 8, 9, and 10; it is clear that the mixtures with different modifiers show different fatigue performance. Based on the data shown in Figures 8 through 10, the number of ESALs required to reach a fatigue cracking failure criteria of 50% area cracked was calculated as shown in Table 13. The mixtures were then ranked based on the ESALs value at the failure criteria. The letter "A" denotes the most fatigue resistant mixture (i.e. most ESAL applications required to reach 50% area cracked) and the letter "F" denotes the least fatigue resistant mixture. As shown in Table 13, the ranking of mixtures was the same regardless of the thickness of the asphalt layer analyzed. However, as expected, the number of ESALs required to reach the failure criteria increased with an increase in asphalt layer thickness. Overall, the PG64-34 SBS mixture had the best fatigue performance whereas the PG64-22 + GTR had the lowest fatigue performance.

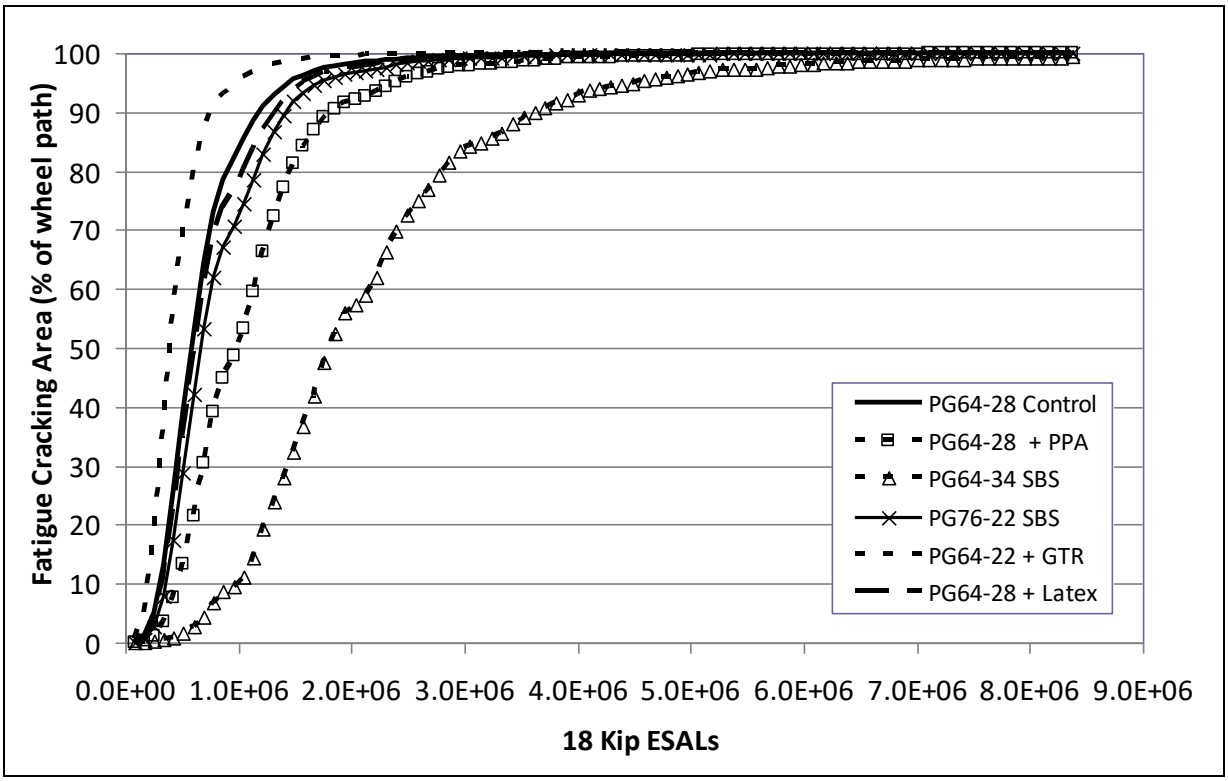

Figure 8. Fracture Mechanics Analysis Results - 50 mm Layer Thickness

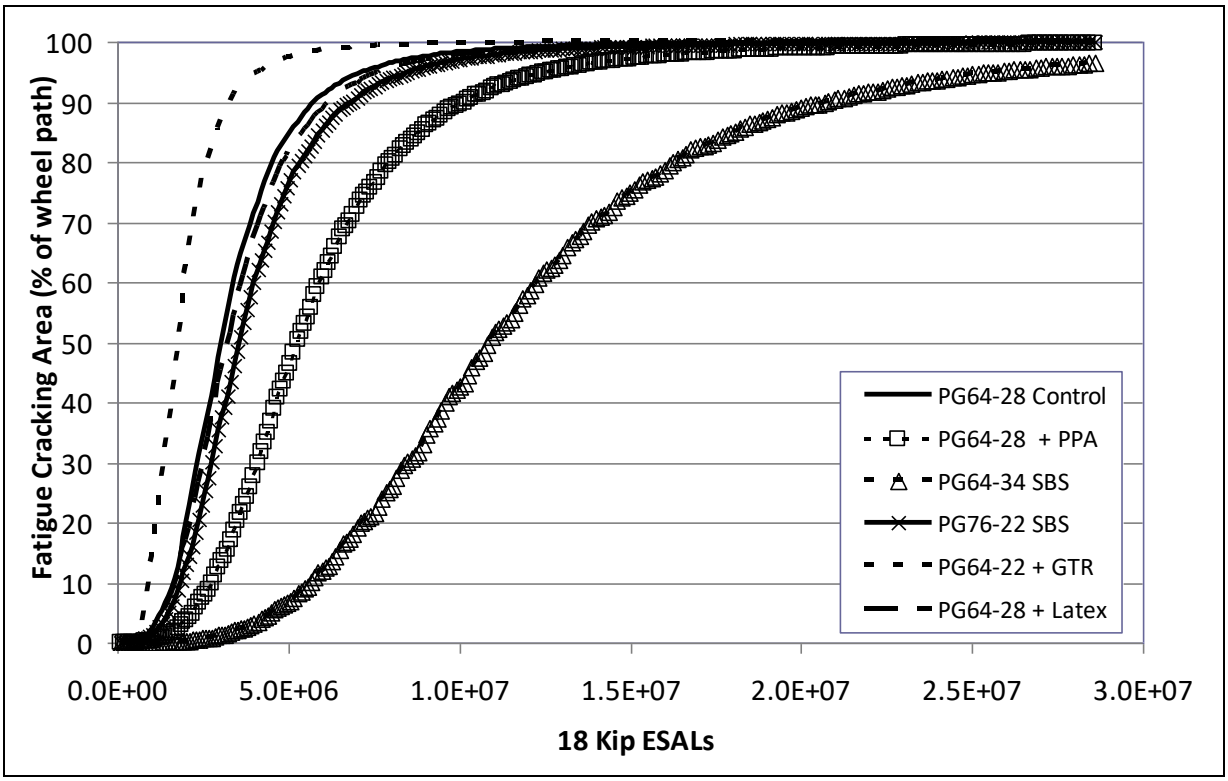

Figure 9. Fracture Mechanics Analysis Results - 100 mm Layer Thickness

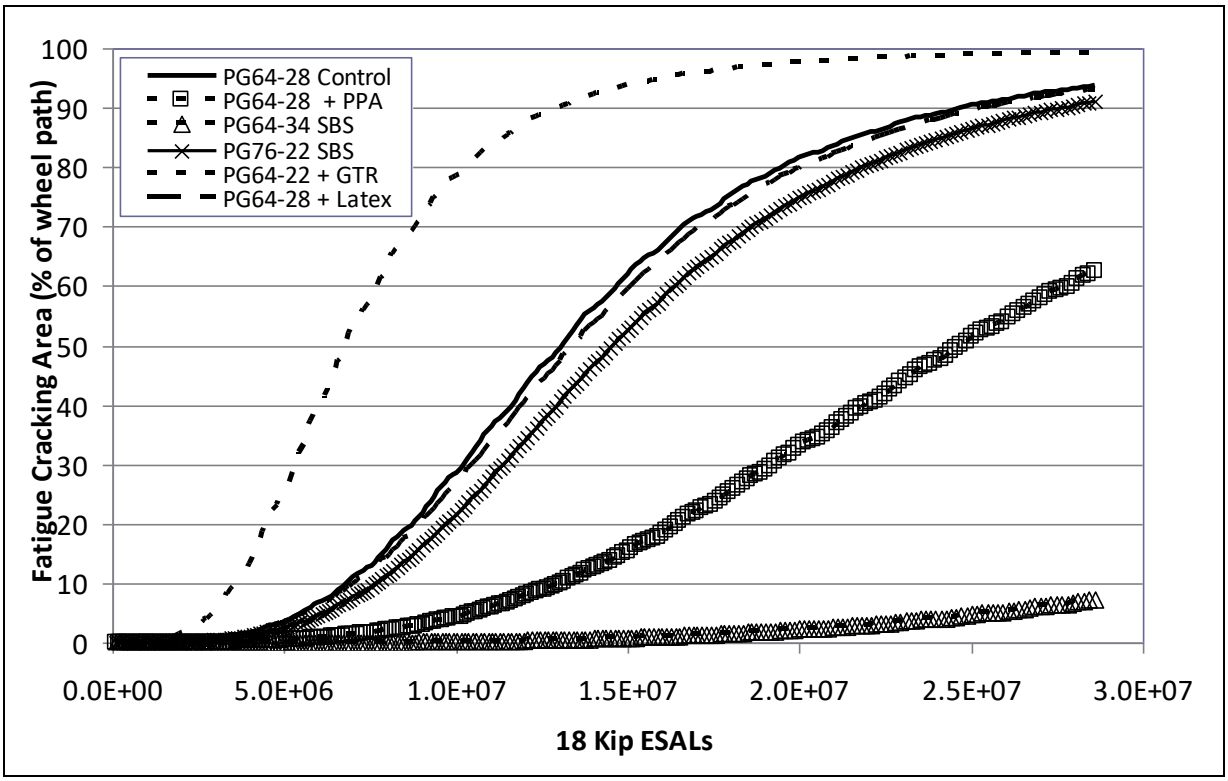

Figure 10. Fracture Mechanics Analysis Results - 150 mm Layer Thickness

Table 13. OT based Fracture Mechanics Prediction of ESALs Resulting in 50% Fatigue Cracking Area

Rank	Binder	50 mm Asphalt Layer	100 mm Asphalt Layer	150 mm Asphalt Layer
E	PG64-28 Control	583,246	3,040,824	13,085,521
B	PG64-28 + PPA	980,633	5,253,184	24,656,389
A	PG64-34 SBS	1,805,996	10,848,760	>28,000,000
C	PG76-22 SBS	664,059	3,573,670	14,544,912
F	PG64-22 + GTR	400,522	1,780,856	6,762,368
D	PG64-28 + Latex	608,113	3,273,376	13,384,886

Note: Letters represents ranking of mixtures fatigue cracking performance with "A" denoting the mixture requiring the most ESAL applications to reach 50% area cracked (i.e. most fatigue resistant).

4.0 Viscoelastic Continuum Damage (VECD) Approach

The VECD-based analysis of asphalt mixtures for fatigue cracking potential has been gaining wide acceptance for the last 10 years (*10*,*11*,*33*,*34*,*35*,*36*). The VECD-based analysis of asphalt concrete was first introduced by Kim and Little (*37*). The theory was originally based on the Shapery's elastic-viscoelastic correspondence principle and work potential theory (*13*). It states that nonlinear behavior caused by distributed micro cracks is accounted by use of the so-called "internal state variables" which define the damage growth within the specimen. There are three primary pseudo-parameters in this technique: (1) pseudostrain (ε^R) is equivalent to linear viscoelastic stress, (2) pseudostiffness (C) represents the reduction in modulus and damage parameter (S) quantifies the micro crack development

within the specimen. For a given time, stress, strain history, following equations are used to calculate these parameters:

$$\varepsilon^R = \frac{1}{E^R}\int E(t-\tau)\frac{\partial \varepsilon}{\partial \tau}d\tau \quad \text{(EQN. 8)}$$

$$\sigma = \frac{\partial W^R}{\partial \varepsilon^R} = I\,C(S)\,\varepsilon^R \quad \text{(EQN. 9)}$$

$$W^R = \frac{I}{2}\,C(S)\,\varepsilon^{R\,2} \quad \text{(EQN. 10)}$$

$$\frac{dS}{dt} = \left(-\frac{\partial W^R}{\partial S}\right)^{\alpha} \quad \text{(EQN. 11)}$$

where ε^R is the pseudostrain, E^R is a reference modulus (often taken as unity), $E(t)$ is the linear viscoelastic relaxation modulus , t is time, τ is the (time) variable of integration, σ is the stress, W^R is the pseudostrain energy density function, $C(S)$ is the pseudostiffness that is assumed to be a function of a single damage parameter S, I is an initial stiffness parameter used to eliminate sample to sample variability and α is a material constant related to the rate of damage growth and equal to inverse of the maximum slope of the log(E(t)) – log(t) curve.

The primary difficulty in evaluating VECD equations stems from the convolution integral given in Equation 8, which is computationally expensive. In order to simplify and promote the practicality of VECD formulations, several researchers derived simplified formulations for the specific cases of cyclic tests with constant frequency (*10,11,12,15,38*). In this paper, the analyses is performed using two different methods of simplified VECD formulations: Method -1, herein called *Incremental* N_f presented by Kutay et al. (*36*) and Method 2, herein called *Reduced Cycles* approach introduced by Christensen and Bonaquist (*12*).

4.1 Method-1: Incremental Nf

In this method, dynamic modulus (|E*|) and uniaxial cyclic push-pull (compression – tension) tests are conducted on HMA samples using the Asphalt Mixture Performance Tester (AMPT). Once the |E*| master curve is developed, a single push-pull test (either stress or strain controlled) at a selected frequency and temperature is sufficient to calibrate the model (i.e., C versus S relationship). However, in order to double check the collapse of C versus S curves at different loading conditions, it is suggested to run the tests at two different temperatures (e.g., 10°C and 20°C) at a selected frequency (e.g., f =10Hz). The summary of this method is as follows:

1. Perform |E*| tests using AASHTO TP62 protocol and develop |E*| master curve.
2. Calculate E(t) master curve through inter-conversion (*38*) and calculate α.
3. Perform push-pull tests and using the peak-to-peak values of stresses and strains calculate C and S values at each cycle N using the flowchart shown in Figure 11. Then plot the C versus S curve. If desired, fit a pre-defined curve to C versus S curve, but this step is not required for N_f calculation in Equation 12.
4. Select a failure criterion (e.g., C=0.5, 50% reduction in modulus), strain level, frequency and temperature and calculate N_f using Equation 12 (*36*).

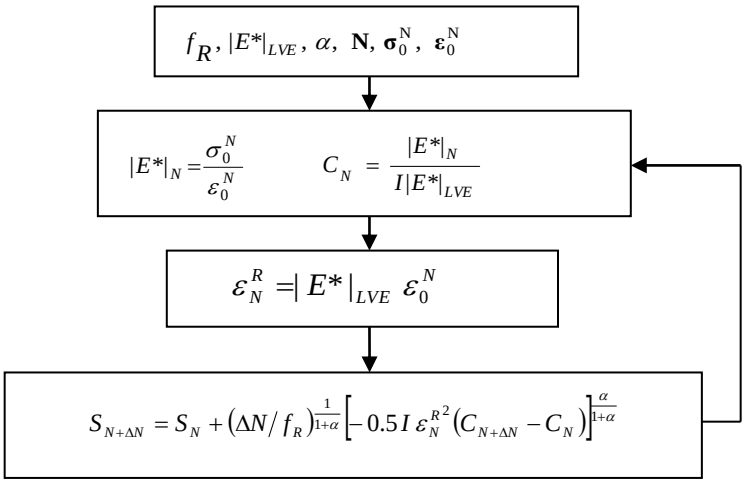

Figure 11. Flowchart for Calculation of C and S at each Cycle N.

$$N_f = \sum_{S=1}^{S_f} \left[-\frac{\varepsilon_0^2 |E^*|_{LVE}^2}{2} \frac{dC}{dS}\Big|_{at\,S} \right]^{-\alpha} f\,\Delta S_S \qquad \text{(EQN. 12)}$$

Steps 1 through 4 are repeated for each HMA mixture and the specimens are ranked based on N_f.

The E(t) master curves and damage exponent (α) values for each specimen tested in this study are shown in Figure 12. Damage exponent (α) is the reciprocal of the maximum slope of the log (E(t))-log(t) curve shown in Figure 12. The pseudostiffness (C) versus damage parameter (S) curves of the specimens are shown in Figure 13, which indicate significant differences between different HMA types. However, it should be noted that the mixtures should not be ranked based on the C versus S curve. Instead, number of cycles to failure (e.g., 50% reduction in stiffness(C=0.5)) should be calculated at different strain levels and temperatures.

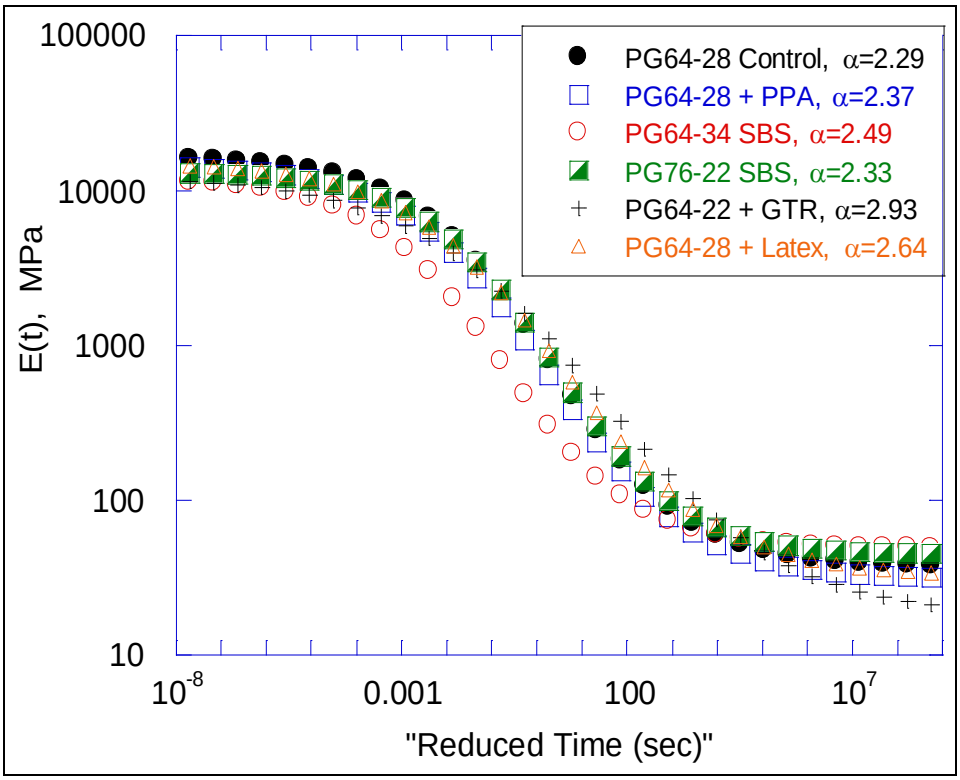

Figure 12. E(t) Master Curves of HMA Specimens.

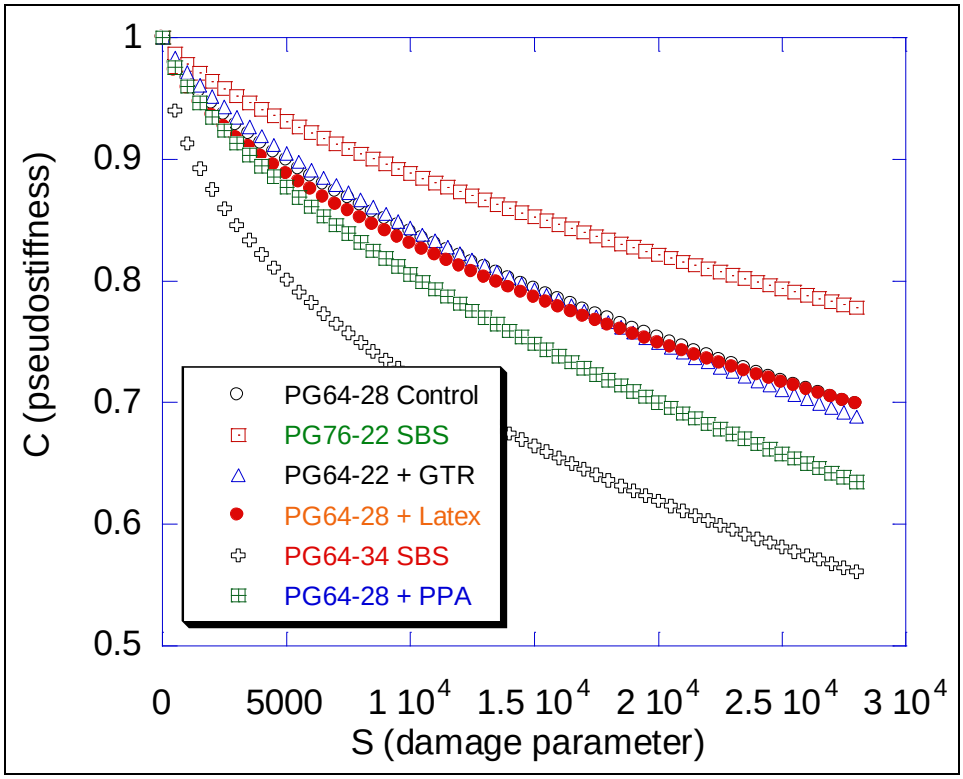

Figure 13. Damage Characteristic Curves of the Mixtures.

In order to mimic the only standardized HMA fatigue test (AASHTO T321 beam fatigue protocol [*1*]), fatigue lives (i.e., N_f) of the HMA mixtures were calculated at four different strain levels (i.e., 75, 175, 350 and 500 micro strain amplitude, i.e., half peak) and at two temperatures (15ºC and 25ºC) as shown in Figure 14. As expected, the N_f decreases with increasing strain level and with decreasing temperature (when Figures 14(a) and (b) are compared).

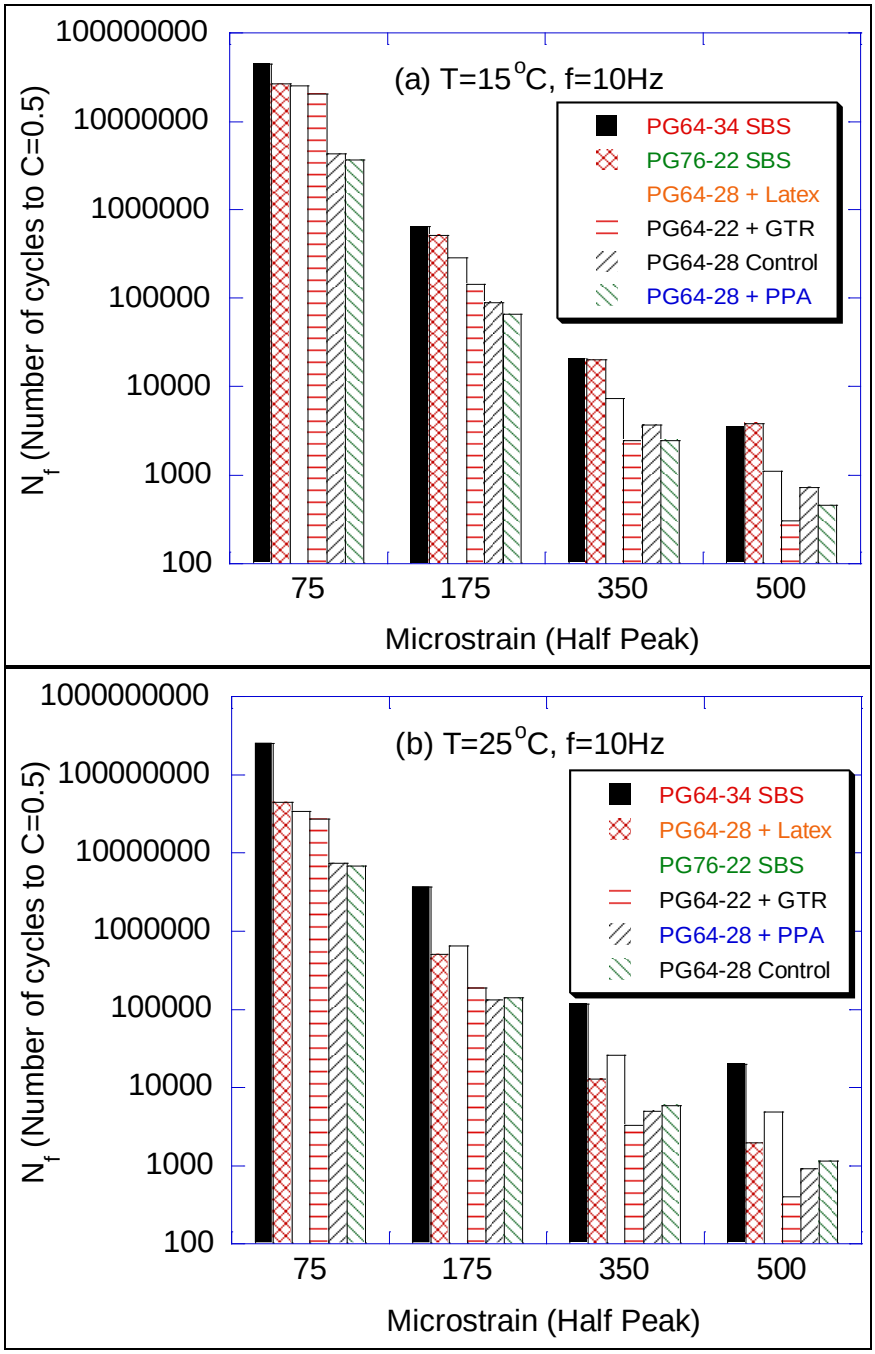

Figure 14. Fatigue Lives of Different Mixtures at Four Strain Levels (i.e., 75, 175, 350 and 500 micro strain amplitude, i.e., half peak) and at Two Temperatures; (a) 15ºC and (b) 25ºC.

Results indicated that the polymer modified mixtures PG63-34 SBS, PG76-22 SBS and PG64-28 + Latex have higher N_f (i.e., better performance) as compared to PG64-28 Control, PG64-28 + PPA modified and

PG64-22 + GTR mixtures. This finding was similar to the binder testing statistical rankings shown in Tables 10 and 11. The ranking of the mixtures slightly change with change in strain level and temperature. For example, in Figure 14a, when the N_f s at 175 and 500 micro strain are compared, PG64-22 + GTR moves from 4th rank to 6th, and PG76-22 SBS and PG64-34 SBS interchange ranking.

4.2 Method-2: Reduced Cycles

The concept of *reduced cycles* has been recently introduced by Christensen and Bonaquist (*11,12).* This method does not utilize the damage parameter (S), instead, it defines a different damage characteristic curve which is C (pseudostiffness, C= $|E^*|/|E^*|_{LVE}$ for cyclic tests with constant frequency) versus N_R (reduced cycles). The reduced cycles, N_R, is computed using the following formula (*12*):

$$N_R = N_{R-ini} + N\left(\frac{f_0}{f}\right)\left(\frac{|E^*|_{LVE}}{|E^*|_{LVE/0}}\right)^{2\alpha}\left(\frac{\varepsilon^E}{\varepsilon_0^E}\right)^{2\alpha}\left[\frac{1}{a(T/T_0)}\right] \qquad \text{(EQN. 13)}$$

where, N_R=reduced cycles, $N_{R\text{-}ini}$ = initial value of reduced cycles, prior to the selected loading period, N = actual loading cycles, f_0 = reference frequency (10 Hz suggested), f = actual test frequency, $|E^*|_{LVE}$ = initial (linear viscoelastic or LVE) dynamic modulus under given conditions, $|E^*|_{LVE/0}$ = reference initial (LVE) dynamic modulus, lb/in^2 (the LVE modulus at 20°C is suggested), α = continuum damage material constant, ε^E = effective applied strain level (equals to applied strain minus the endurance limit strain, ε_0^E = reference effective strain level (0.0002 suggested), $a(T/T_0)$ = shift factor at test temperature T relative to reference temperature T_0.

In this method, dynamic modulus master curve is not used. Instead, an initial $|E^*|_{LVE}$ is assumed based on the initial value of the measured |E*| during the test. It can also be measured at the beginning of the test by applying low strain level, at the expense of risking possible initial damage to the specimen. In addition, the damage parameter (α) is not computed from E(t) master curve and is assumed to be constant (typically assumed to be 2.0). The advantage of not using |E*| master curve is elimination of requirement of AASHTO TP62 test; however, the disadvantage is that the user needs to decide on the values of $|E^*|_{LVE}$ and α, which makes the model prone to user-dependency and introduces empiricism. In addition, with this technique, user needs to decide on the endurance limit to bring the C versus N_R curves of different temperatures and strain levels together.

Detailed description of this method is given elsewhere (*12*), therefore it will not be repeated here. However, a brief description of the summary of the method is as follows:

1. Perform push-pull fatigue tests at two temperatures (e.g., 20C and 4C) at two strain levels.
2. Select reference conditions, e.g.: $|E^*|_{LVE/0} = 2.9\text{x}10^5$ psi, $\varepsilon_0^E = 0.0002$, $f_0 = 10$Hz.
3. Calculate C ($=|E^*| / |E^*|_{LVE}$) and N_R (Equation 13) at each cycle for each test.
4. Define Y = ln($C^{-1} - 1$) and X = ln(N_R), and plot the Y versus X curve, which should be linear.
5. Fit a linear line to the Y versus X curve and determine the *A* and *B* constants for Y = *A* + *B*X.
6. Determine $K_1 = \exp(-A)$ and $K_2 = B$, where K_1 represents number of cycles to 50% reduction in stiffness (i.e., fatigue half-life).
7. Repeat steps 3 through 6 for each test temperature and strain level.
8. Adjust values of endurance limit and if necessary $|E^*|_{LVE}$ at each test temperature and strain level to bring the Y versus X curves together into single line.
9. Record K_1 and K_2 value for the given mixture.

Different HMA specimens can be ranked using K_1 (i.e., fatigue half-life). In addition, cycles to failure at different temperatures and strain levels (but not at different frequencies) can be computed by a simple rearrangement of Equation 13 and by use of K_1 and K_2.

Table 14 shows the K_1 and K_2 coefficients of mixtures tested in this study. Figure 15 shows the C versus reduced cycles (N_R) relationship of the mixtures tested in this study which are computed using the following formula (*12*):

$$C = \frac{1}{1+\left(N_R/K_1\right)^{K_2}} \qquad \text{(EQN. 14)}$$

Table 14. K_1 and K_2 Coefficients of Mixtures Tested in this Study.

Specimen	K_1	K_2
PG64-34 SBS	18882364	0.207
PG64-28 + Latex	8410323	0.276
PG64-28 + PPA	829214	0.306
PG76-22 SBS	764119	0.323
PG64-22 + GTR	391895	0.247
PG64-28 Control	110722	0.335

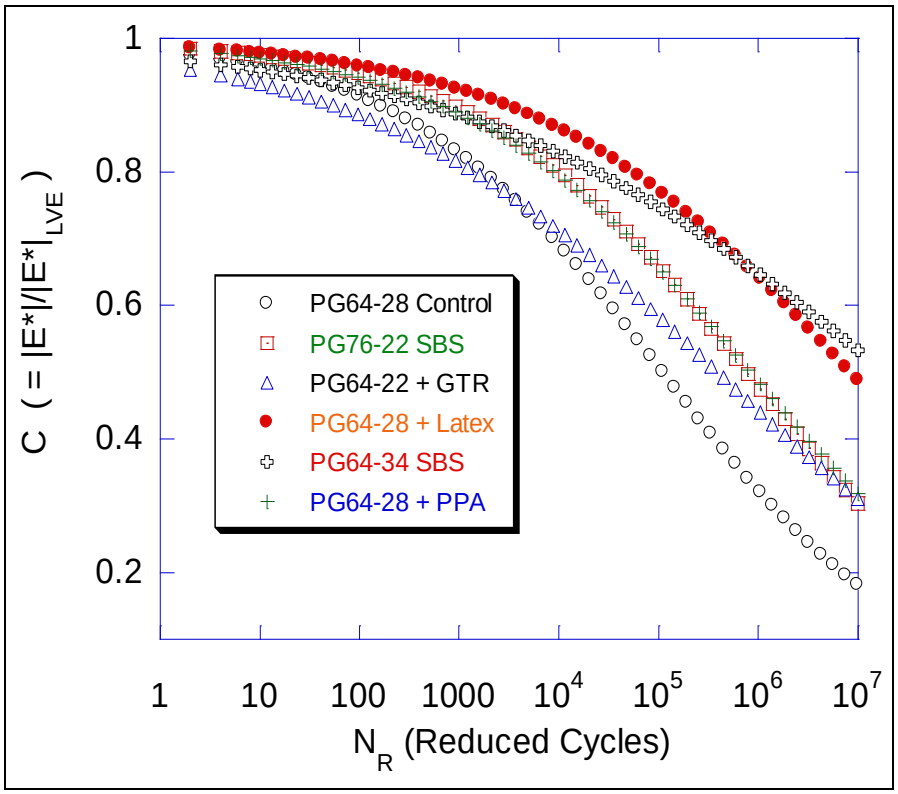

Figure 15. Stiffness Reduction (= C) versus Reduced Cycles (N_R) Relationship of the Mixtures Tested in this Study.

Figure 16 shows the number of cycles to failure (N_f) of the mixtures computed using the Reduced Cycles approach. In this figure, the plot sequence of the specimens has been kept the same as the ones in Figure 14 to facilitate comparison. Similar to Figure 14, Figure 16 also indicates that the polymer modified mixtures PG64-34 SBS, PG64-28 + Latex and PG76-22 SBS perform better than other mixtures at strain levels larger than 175 micro strain. At low strain level (i.e., 75 micro strain), PG64-28 Control and PG64-28 + PPA modified binder seems to have large N_f.

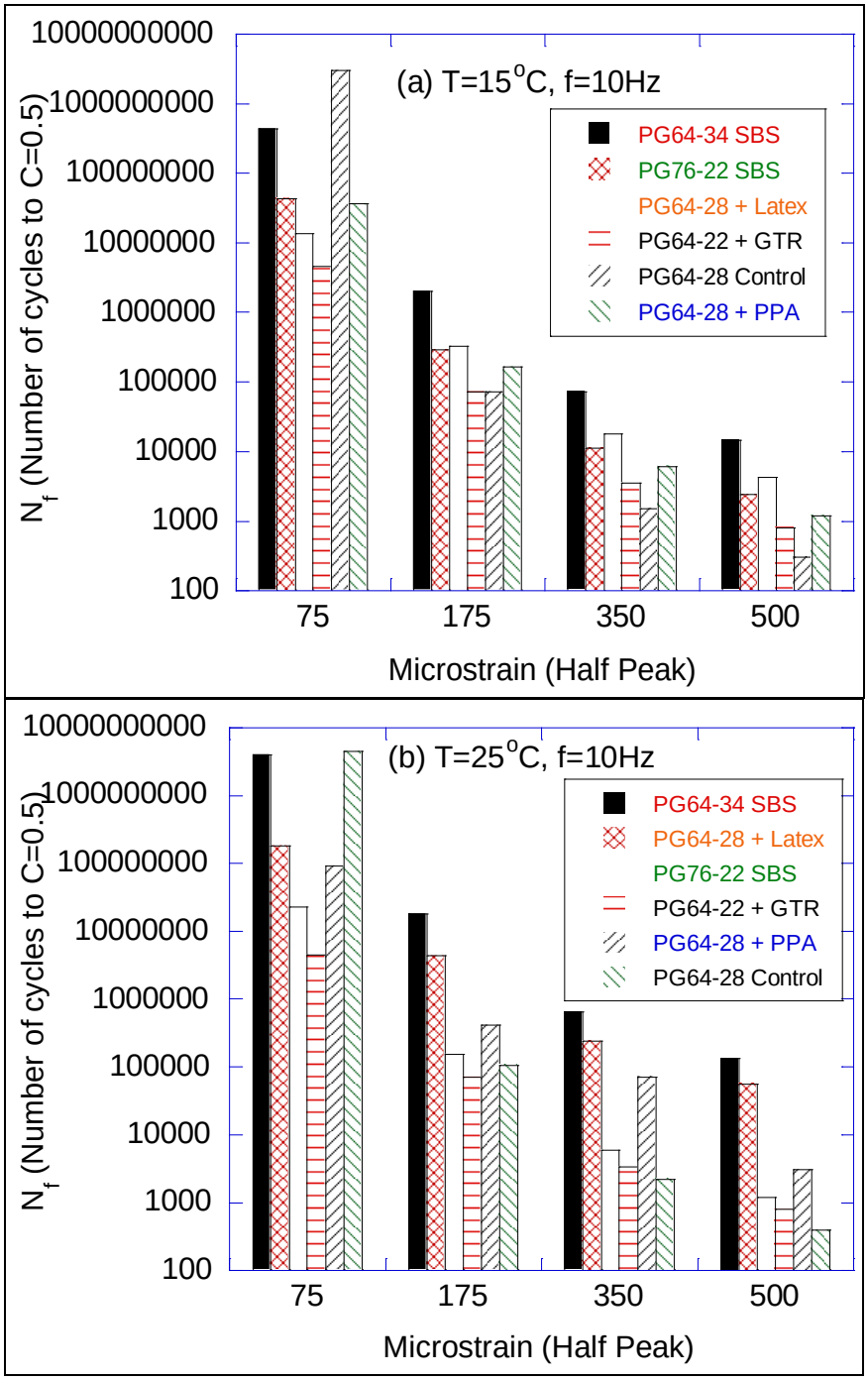

Figure 16. Fatigue Lives of Different Mixtures Computed using Method-2: Reduced Cycles, at Four Strain Levels (i.e., 75, 175, 350 and 500 micro strain amplitude, i.e., half peak) and at Two Temperatures; (a) 15ºC and (b) 25ºC.

Chapter Four: Effect of Binder Type, Mastic, and Aggregate Type on the Low Temperature Characteristics of Modified Hot Mix Asphalt

1.0 Description of Low Temperature Cracking Simple Performance Tests For Binder and Mixture

1.1 Asphalt Binder Cracking Device (ABCD)

The ABCD uses the dissimilar coefficients of thermal expansion/contraction (CTE) of asphalt binders and metals to directly determine the cracking temperature of asphalt binders. As shown in Figure 17, the ABCD consists of a hollow cylindrical metal ring with a uniform thickness and an electrical strain gauge glued to the inside of the ring. The ABCD ring has an outside diameter of 50 ± 0.05 mm, a height of 13.72 ± 0.05 mm, and a thickness of 1.65 ± 0.05 mm. A temperature sensor is also glued to the inside of the ring assembly to closely monitor the specimen temperature. The asphalt binder is molded onto the outside of the ABCD ring as shown in Figure 17.

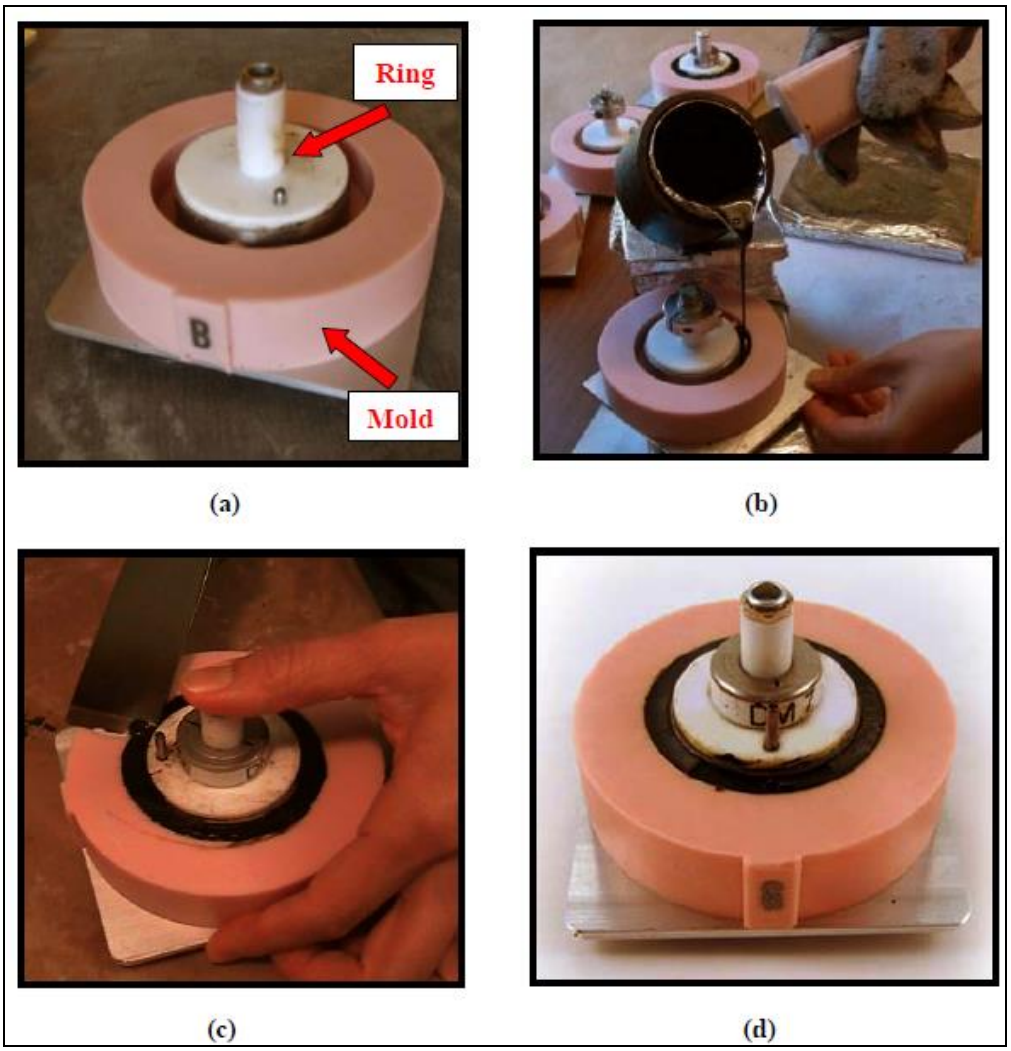

Figure 17. ABCD Specimen Preparation - (a) ABCD mold and strain gage ring (b) pouring binder into mold (c) specimen trimming (d) specimen ready for testing.

Since asphalt binders have much larger coefficients of thermal expansion/contraction than do metals, the differential thermal contraction (more rapid contraction of asphalt binder than metal) will cause development of tensile stress in the asphalt as the temperature is reduced. This accumulation of tensile stress will eventually lead to thermal cracks. Strain in the metal ring caused by the thermal stress is measured by an electrical strain gauge and used to calculate fracture stress of the asphalt binder. When the specimen cracks, the accumulated thermal stress is relieved and will be shown as a sudden drop in the strain reading. The cracking temperature of the asphalt binder is directly determined as the temperature where the sudden drop of measured strain occurs.

1.2 Asphalt Concrete Cracking Device (ACCD)

The ACCD uses a similar test configuration with a larger scale as compared to the ABCD (*19*). For this test, a circular shaped asphalt mixture specimen is compacted around a circular thermal stress restraining device located in the middle of the asphalt mixture. The compacted asphalt mixture specimen and thermal stress restraining device are tested together.

The ACCD inner ring (thermal stress restraining device) is made of an Invar, a steel alloy with the coefficient of thermal expansion/contraction (CTE) of 2.0x10-6/°C or less at the testing temperature range. This ring is instrumented with a strain gage rosette and a temperature sensor on the inside wall. A 254 mm (10 in.) diameter and 63.5 mm (2.5 in.) height sample is then compacted around this ring as shown in Figure 18. The cross-section of sample, 76.2 mm (3 in.) x 63.5 mm (2.5 in.), allows for testing mixtures with the common size of aggregates used in surface HMA.

For the ACCD a circular asphalt specimen is fabricated as shown in Figure 18. Each specimen requires approximately 6,000 g (13 lb) of loose asphalt mixture. The heated loose mixture is aged for four hours at 135°C as outlined in AASHTO R30 "Mixture Conditioning of Hot Mix Asphalt (HMA)"(*1*) prior to compaction. The heated loose mixture is introduced into the mold assembly (Figure 18a & 18b) which has also been heated to the compaction temperature. The loose mix is then rodded 40 times with a spatula (Figure 18c) and subsequently the surface is smoothed. Next the pressing head is applied to the top of the mold assembly as shown in Figure 18d. The mold assembly is then placed into a compression machine (Figure 18e) and the loose mixture compacted by applying a load of 445 kN (100,000 lb) load to the pressing head. Once, the target load is achieved, the load is held for 15 seconds and then removed. The loading and unloading process is completed a total of three times. The target air void content is 9 + 1% - this air void level was selected to minimize crushing of the aggregates under load (*19*). The sample is then allowed to cool for 2 hours or more before it is extracted from the mold. The extracted samples are then allowed to cool overnight.

Next a 38.1 mm (1.5 in.) notch is cut into on the compacted sample using a dry circular saw. The width of the notch is generally 4 mm. This notch is located on the outer diameter of the specimen (Figure 18f) and is aligned with strain gage installed in ACCD inner ring. The purpose of the notch is to address the limitations associated with predicting true fracture properties of un-notched samples. These limitations are primarily related to the initiation and propagation mechanisms of the cracks (*21*). Since the asphalt mixture specimens do not have ends, no additional specimen preparation (coring, gluing or instrumentation) is required. The notched sample is then placed inside an environmental chamber and the strain and temperature sensors connected to the data acquisition system (Figure 18g). After preconditioning at 0°C (32°F) for one hour, the sample is then cooled at 10°C/hour rate to -60°C (-76°F) or until fracture occurs. The strain and temperature sensor readings are recorded throughout the test.

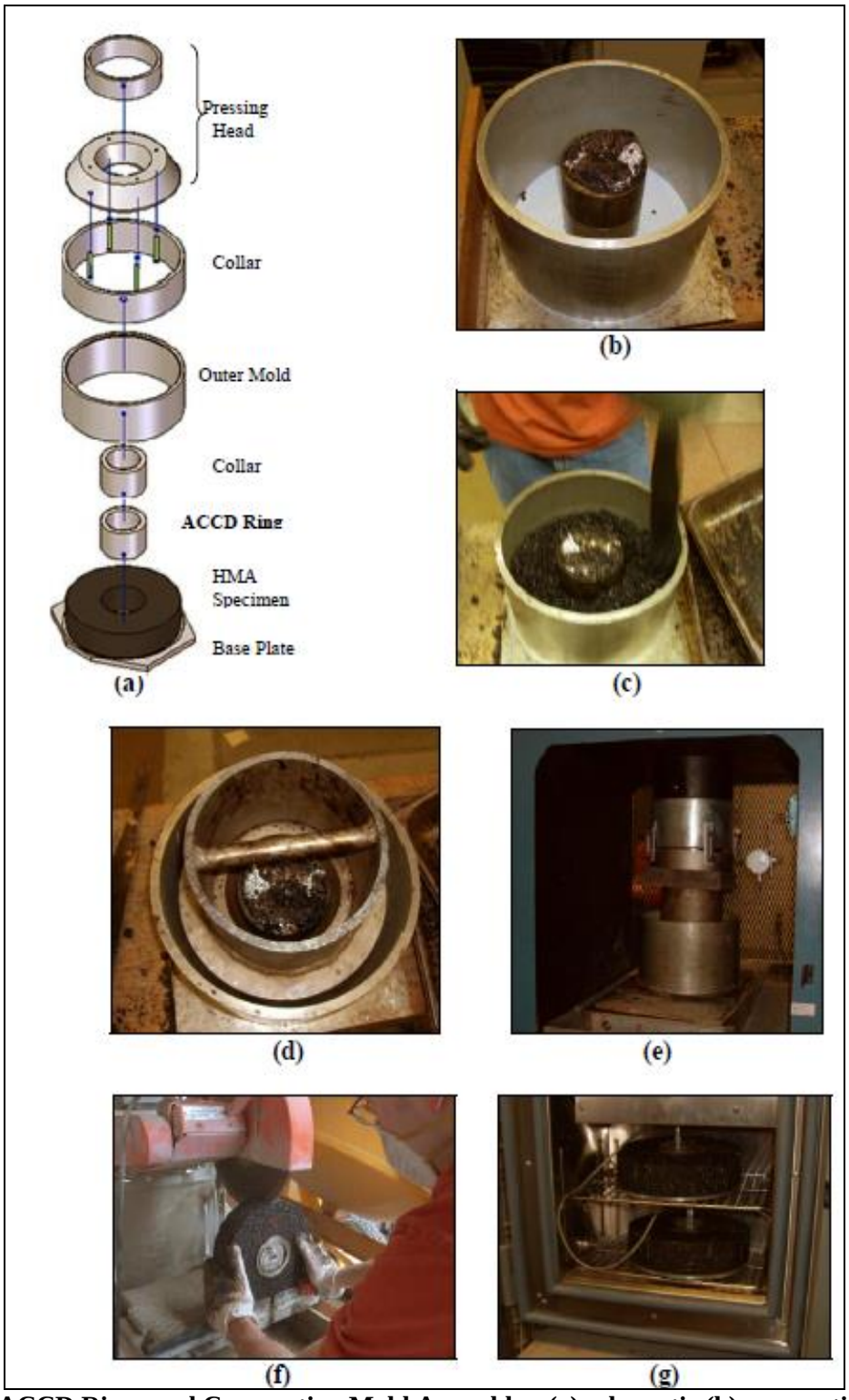

Figure 18. ACCD Rings and Compaction Mold Assembly - (a) schematic (b) compaction setup (c) rodding of mixture (d) pressing head placed on specimen (e) compaction with a static compression machine (f) cutting notch in specimen (g) compacted samples with an ACCD ring ready for testing.

As the temperature inside the environmental chamber is lowered, the asphalt mixture attempts to contract. This contraction is prevented by the presence of the ACCD ring which causes tensile stress in the sample

and compression in the ACCD ring. This specimen continues to accumulate stress until it breaks. After the test, a plot of strain (resulting from the thermal tensile stress on the ACCD ring) versus temperature are constructed to determine the ACCD cracking temperature. As shown in Figure 19, lines are drawn tangent to the initial linear portion and the final linear portion of the strain versus temperature curve. The temperature where these two lines intersect is the cracking temperature for such mixes.

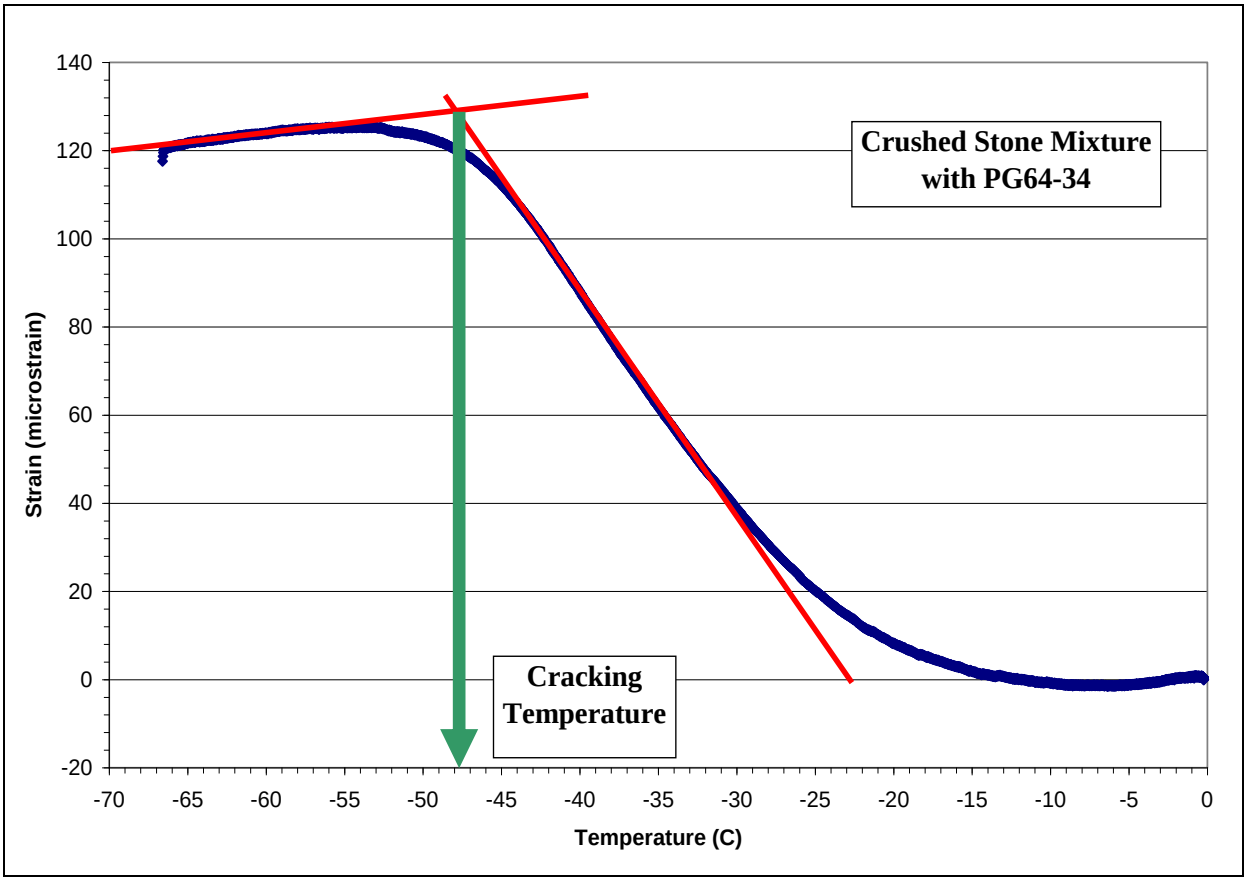

Figure 19. Example of Graphical Procedure for Determining ACCD Cracking Temperature from Transient Failure.

For this study, two ACCD specimens were compacted and simultaneously tested per day. After the completion of the test, each sample was cut into two halves and the air voids of each half was measured following AASHTO T166. The average air voids of all the tested specimens ranged from 8.0 to 9.5 percent.

2.0 Data and Analysis

The continuous low temperature grade and critical cracking temperature (T_{cr}) of each binder are presented in Table 15. The cracking temperatures of the binders and mastics using the ABCD and the cracking temperatures of the mixtures using the ACCD are presented in Table 16. Figure 20 presents a comparison of all the binder data, mastic data, and mixtures data.

Eight sets of data were correlated to each other by calculating the Pearson product moment correlation coefficient (r). Typically, r value ranges from +1.0 to -1.0. The larger the absolute magnitude of r, the stronger the degree of linear relationship. Table 17 presents the r values for the correlations of the eight sets of data.

Table 15. Continuous Grade Low Temperature & AASHTO Critical Cracking Temperature Results

Binder	Continuous Grade Low Temp., ºC	Critical Cracking Temp. (T_{cr}) ºC
PG64-28 Neat Binder	-29.2	-28.4
PG64-28 + PPA	-29.6	-28.9
PG64-34 SBS	-36.1	-36.3
PG76-22 SBS	-27.6	-25.1
PG64-28 + Latex	-26.3	-25.7
PG64-22 + GTR	-19.8	-24.7

Table 16. ABCD & ACCD Results

Binder	ABCD Binder Testing		ABCD Mastic Testing		ACCD Mixture Testing	
	Unaged	Aged	Crushed Stone	Gravel	Crushed Stone	Gravel
PG64-28 Neat Binder	-34.5	-31.7	-39.5	-42.2	-32.3	-32.8
PG64-28 + PPA	-36.8	-35.7	-40.4	-42.0	-34.3	-35.0
PG64-34 SBS	-43.3	-43.3	-48.9	-49.0	-47.5	-48.0
PG76-22 SBS	-36.0	-33.2	-36.8	-38.8	-35.3	-35.8
PG64-28 + Latex	-36.0	-31.5	-36.7	-37.3	-32.0	-32.5
PG64-22 + GTR	-38.4	-32.6	-36.5	-38.6	-36.8	-40.0

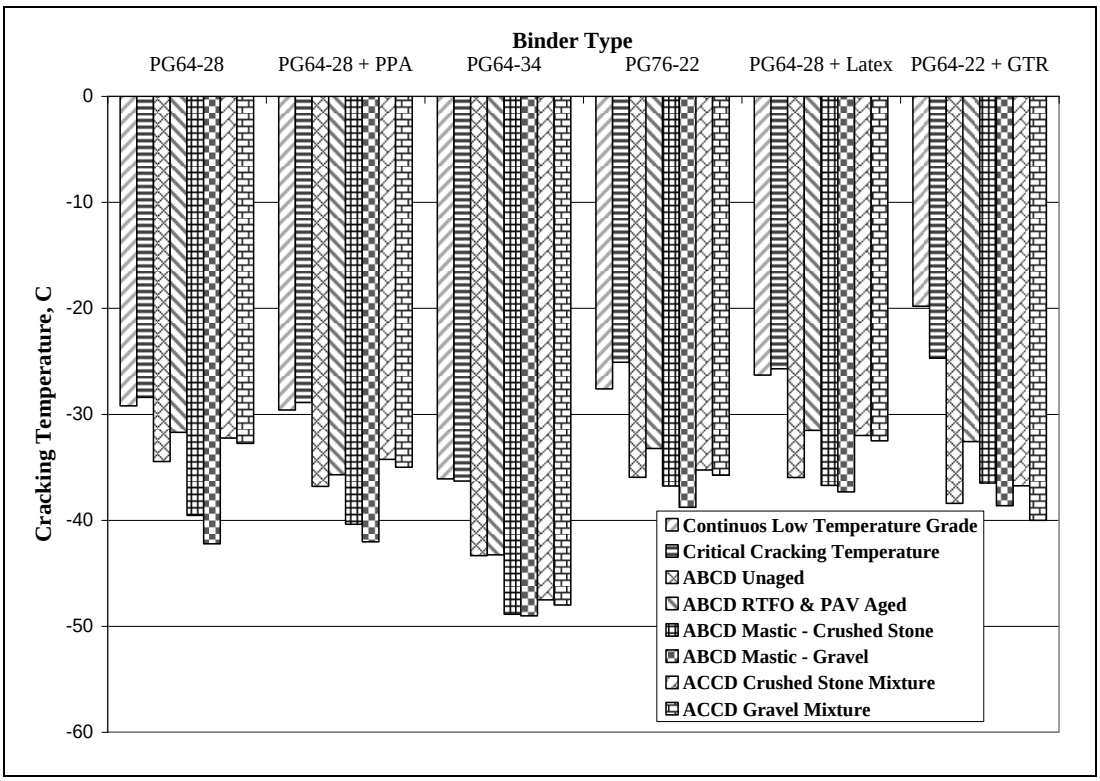

Figure 20. Comparison Between Binder Grade, Critical Cracking Temperature, ABCD Binder and Mastic Testing Results, and ACCD Mixture Testing Results.

The low temperature cracking of the unaged and aged binders measured using the ABCD provided better correlation than T_{cr} to the low temperature cracking of the mixtures measured using the ACCD. This was true for the crushed stone and gravel mixtures. Unaged binder tested in the ABCD correlated better with ACCD mixture tests than the ABCD aged binder tests. This might indicate that the mixtures should have been aged longer or the binders that were only RTFO aged should have been tested. Finally, comparison of the ABCD mastic and ACCD mixture test results showed that the effect of aggregates on low temperature cracking is very consistent with the gravel performing better than crushed stone aggregates

Since the PG64-34 binder tested exhibited exceptionally low cracking temperatures, its' data might have skewed the overall data set and affected the statistical analysis. Regressions and correlation of the low temperature cracking of the mixtures to the T_{cr}, low temperature cracking of the unaged binders, and the low temperature cracking of the aged binders were made for two sets of data (one with and without the PG 64-34). There were no significant differences in the trends between the two sets of data and therefore the data trends were not skewed.

Table 17. Pearson Correlation Statistical Analysis of Results

	Cont. Low Temp. Grade	**AASHTO Critical Cracking Temp., T_{cr}**	**ABCD (unaged)**	**ABCD (aged)**	**ABCD Crushed Stone Mastic**	**ABCD Gravel Mastic**	**ACCD Crushed Stone**	**ACCD Gravel**
Cont. Low Temp. Grade	1	0.861[a]	0.480	0.764	0.879[a]	0.820[a]	0.557	0.422
AASHTO Critical Cracking Temp, T_{cr}	-[c]	1	0.775	0.936[b]	0.993[b]	0.961[b]	0.810	0.730
ABCD (unaged)	-	-	1	0.920[b]	0.764	0.743	0.964[b]	0.960[b]
ABCD (aged)	-	-	-	1	0.929[b]	0.914[b]	0.922[b]	0.869[a]
ABCD Crushed Stone Mastic	-	-	-	-	1	0.971[b]	0.827[a]	0.744
ABCD Gravel Mastic	-	-	-	-	-	1	0.828[a]	0.765
ACCD Crushed Stone	-	-	-	-	-	-	1	0.987[b]
ACCD Gravel	-	-	-	-	-	-	-	1

[a] = Correlation is significant at the 0.05 level. [b] = Correlation is significant at the 0.01 level.
- = Data not presented since correlation is symmetric.

Chapter Five: Conclusions & Recommendations

Based on the data collected and the data analysis, the following conclusions were made:

- The elastic recovery on unaged and aged binders and the Multiple-Stress Creep Recovery (MSCR) tests showed that the binders that had modification yielded higher elastic recovery values and higher percent recovery values in the MSCR test. The PG64-34 SBS had the highest elastic recovery among the binders tested.

- Rankings from the binder tests showed that the modified binders performed better than the non-modified binders in terms of elastic recovery with the PG64-34 SBS, PG76-22 SBS and PG64-28 + Latex performing better than the PG64-28 Control and PG64-28 + PPA.

- The OT based fracture mechanics approach showed that different modified asphalt binders have different fatigue performance. This was based on a 50% area cracked failure criteria. Also, the statistical ranking of the asphalt modified binders based on elastic recovery and percent recovery were different than the rankings of the mixtures based on the mentioned failure criteria.

- The linear viscoelastic continuum damage analysis utilizing the incremental N_f by Kutay showed that mixtures with modified asphalt binders have better fatigue performance than the PG64-28 Control and the PG64-28 + PPA, however, with the exception at the higher micro strain level where the PG64-22 + GTR performed worse than the PG64-28 Control and the PG64-28 + PPA. Generally, this approach ranked the mixtures similar to the statistical ranking of the elastic recovery and percent recovery of the asphalt binders at low strain levels.

- The linear viscoelastic continuum damage analysis utilizing the reduced cycles method by Don Christensen showed that the PG64-34 SBS and the PG76-22 SBS performed better than the rest of the modified binders at the higher micro strain levels. However, at the lower strain levels, the method showed that the PG64-28 Control would perform better in terms of the fatigue than the modified binders. Generally, the exact ranking of the mixtures based on this approach was not similar to the ranking of the binders.

- Overall the rankings between the two viscoelastic continuum damage analysis methods were generally consistent, with the exception the 75με reduced cycles method, where the PG64-28 Control ranked better than the modified binders. In the remaining cases, the PG64-34 SBS, PG76-22 SBS and PG64-28 + Latex were generally ranked higher than the remaining binders.

- Rankings based on the OT based fracture mechanics approach indicated the same best fatigue performing binder, PG64-34 SBS, as the viscoelastic continuum damage approaches. Also, the mixture rankings between these two methods were similar at higher strain levels.

- Examination of the binder and mixture analysis data showed that the PG64-22 + GTR was a strain sensitive material. The binder data indicated that this binder broke during elongation in the elastic recovery test when pulled to 20 cm but did not break when pulled to 10 cm. Similarly, the OT based fracture mechanics identified the PG64-22 + GTR as the lowest performing of all the binders tested. This was expected because the OT approach focuses on crack propagation and large strain. The binder strain sensitivity was further identified using the viscoelastic continuum damage analysis, which showed that the binders' ranking gradually decreased as the strain level increased.

- For the majority, the rankings (See Tables 18 and 19) established from the binder and mixture tests and analysis showed that the modified binders performed better than the non-modified binders in terms of elastic recovery and mixture fatigue performance. The majority of analyses identified the PG64-34 SBS as the most elastic binder and most fatigue resistance mixture. Thereafter the exact rankings of the binders changed depending on the specific test. The rankings for both the binder tests and mixture tests indicated similar trends; however the trend was not consistent enough to specifically indicate whether the binder elasticity tests wholly describe the fatigue cracking behavior of the mixture.

Table 18. Binder Test Percent Recovery Rankings

	Binders					
Test	**PG64-28 Control**	**PG64-28 + PPA**	**PG64-34 SBS**	**PG76-22 SBS**	**PG64-22 +GTR**	**PG64-28 + Latex**
Binder Test Rankings						
Elastic Recovery AASHTO T301 Unaged	E	D	A	C	No Data	B
Elastic Recovery AASHTO T301 RTFO Aged	D	E	A	B	No Data	C
Elastic Recovery ASTM D6084 RTFO Aged	E	F	A	B	C	D
MSCR Percent Recovery 100 Pa	E	D	A	B	B	C
MSCR Percent Recovery 3200 Pa	E	F	A	B	D	C

Note: Binder tests rankings based on percent recovery with "A" exhibiting the highest recovery.

Table 19. Mixture Fatigue Cracking Resistance Rankings

Test	Binders					
	PG64-28 Control	**PG64-28 + PPA**	**PG64-34 SBS**	**PG76-22 SBS**	**PG64-22 +GTR**	**PG64-28 + Latex**
Mixture Test Rankings						
OT Based Fracture Mechanics	E	B	A	C	F	D
VECD Incremental N_f Method - 75με	F	E	A	C	D	B
VECD Reduced Cycles Method-75με	A	D	B	C	F	E
VECD Incremental N_f Method - 175με	E	F	A	B	D	C
VECD Reduced Cycles Method-175με	E	D	A	C	E	B
VECD Incremental N_f Method - 350με	D	E	A	B	F	C
VECD Reduced Cycles Method-350με	F	D	A	C	E	B
VECD Incremental N_f Method - 500με	D	E	A	B	F	C
VECD Reduced Cycles Method-500με	F	D	A	C	E	B

Note: Mixture test rankings based on fatigue cracking resistance with "A" being the most crack resistant mixture.

- A statistical analysis of the results indicated a strong correlation between the critical cracking temperature of the binders (T_{cr}) determined using current AASHTO M320 Table 2 and ABCD test results for aged binders (RTFO and PAV aged) and mixture mastics (both aggregate sources). The AASHTO M320 critical cracking temperature results and the ACCD low temperature cracking resistance results did not correlate well.

- A comparison of the binder testing results indicated no correlation existed between the binder continuous low temperature grade and the ABCD test results. However, a correlation did exist between the binder continuous low temperature grade, critical cracking temperature of the binders, and ABCD mastic test results.

- A consistently strong correlation existed between the mixture low temperature cracking resistance results obtained in the ACCD test (for both gravel and crushed stone mixtures) and the ABCD binder test results. ABCD results obtained for unaged binder correlated better with ACCD mixture tests than the ABCD aged (RTFO and PAV) binder tests. This potentially indicates that the mixtures should have been aged longer to correlate with the aged binder results or the binders that were only RTFO aged should have been tested. These results suggest the significance of aging on the ABCD tests results.

- ABCD mastic test results showed a correlation to the ACCD mixture test results for the crushed stone mixture, but not the gravel mixture. Because there was not a strong universal correlation between these test results, this suggested that ABCD mastic testing may not be an appropriate indicator of mixture low temperature cracking resistance.

- The effect of aggregates on low temperature cracking resistance was very consistent. A comparison of the ABCD mastic and ACCD mixture test results showed mixtures with the gravel performing better than crushed stone aggregates**.** This suggests that these tests are sensitive to aggregate/mixture type.

- Generally, the ABCD and the ACCD provided cracking resistance temperatures colder than the AASHTO continuous low grade and the critical cracking temperature.

- Binder type had a significant impact on the low temperature cracking resistance of the mixture. The PG64-34 binder definitively performed the best in all the binder tests. Analysis showed that the data was not skewed with the inclusion of the PG64-34 data. This suggested that these tests are sensitive to binder type and can be used to differentiate them based on their low temperature cracking resistance.

References

1. American Association of State Highway and Transportation Officials, Standard Specifications for Transportation Materials and Methods of Sampling and Testing, American Association of State Highway and Transportation Officials (AASHTO), Washington, D.C., 2010.

2. "Annual Book of ASTM Standards" American Society for Testing and Materials (ASTM), Volume 04.03, 2008.

3. "2008 AASHTO Provisional Standards" American Association of State Highway and Transportation Officials (AASHTO), June 2008 Edition.

4. J. D'Angelo, R. Kluttz, R. Dongre, K. Stephens and L. Zanzotto. "Revision of the Superpave High Temperature Binder Specification: The Multiple Stress Creep Recovery Test" Journal of the Association of Asphalt Paving Technologists (AAPT), Vol. 76, 2007.

5. J. D'Angelo and R. Dongre. "Development of a High Temperature Performance Based Binder Specification in the United States" International Society for Asphalt Pavements (ISAP) - 10th International Conference on Asphalt Pavements, 2006.

6. J. D'Angelo, R. Dongre and G. Reinke. "Evaluation of Repeated Creep and Recovery Test Method as an Alternative to SHRP+ Requirements for Polymer Modified Asphalt Binders" Canadian Technical Asphalt Association (CTAA) – 51st Annual Conference, 2006.

7. F. Zhou, S. Hu, T. Scullion, D. H. Chen, X. Qi, and G. Claros. "Development and Verification of the Overlay Tester Based Fatigue Cracking Prediction Approach" Journal of the Association of Asphalt Paving Technologists (AAPT), Vol. 76, 2007.

8. F. Zhou, S. Hu, D.H. Chen, and T. Scullion. "Overlay Tester: A Simple Performance Test for Fatigue Cracking" Transportation Research Record: Journal of the Transportation Research Board, No. 2001, 2007.

9. F. Zhou and T. Scullion. "Overlay Tester: A Rapid Performance Related Crack Resistance Test" Federal Highway Administration, Report No. FHWA/TX-05/0-4467-2, 2005.

10. M.E. Kutay, N.H. Gibson, and J. Youtcheff. "Conventional and Viscoelastic Continuum Damage (VECD) based Fatigue Analysis of Polymer Modified Asphalt Pavements" Journal of Association of Asphalt Paving Technologists, Vol. 77, 2008.

11. D. W. Christensen and R. F. Bonaquist. "Practical Application of Continuum Damage Theory to Fatigue Phenomena in Asphalt Concrete Mixtures" Journal of Association of Asphalt Paving Technologists, Vol.74, 2005.

12. D. Christensen R. Bonaquist "Analysis of HMA Fatigue Data Using the Concepts of Reduced Loading Cycles and Endurance Limit" Journal of Association of Asphalt Paving Technologists, 2009 (In-press).

13. R.A. Schapery "Correspondence Principles and a Generalized J-Integral for Large Deformation and Fracture Analysis of Viscoelastic Media" International Journal of Fracture, Vol. 25, 1984.

14. J.S Daniel, W. Bisirri, and Y.R. Kim. “Fatigue Evaluation of Asphalt Mixtures using Dissipated Energy and Viscoelastic Continuum Damage Approaches” Journal of the Association of Asphalt Paving Technologists (AAPT), Vol. 73, 2004.

15. J.S Daniel and Y.R. Kim. “Development of a Simplified Fatigue Test and Analysis Procedure Using a Viscoelastic, Continuum Damage Model” Journal of the Association of Asphalt Paving Technologists (AAPT), Vol. 71, 2002.

16. H.J. Lee, Y. R. Kim and S. W. Lee. “Prediction of Asphalt Mix Fatigue Life with Viscoelastic Material Properties” Transportation Research Record: Journal of the Transportation Research Board, No. 1832, 2003.

17. C. L Monismith,, G. Secor, and K.E.Secor “Temperature Induced Stresses and Deformations in Asphalt Concrete,” Journal of the Association of Asphalt Paving Technologists, Vol. 34, 1965, pp. 248-285.

18. T. Vinson, V. Janoo, R. and Haas. “Summary Report on Low Temperature and Thermal Fatigue Cracking,” Strategic Highway Research Program-A-306, National Research Council, Washington, D.C. 1989.

19. S. Kim, A. Wargo, A. and D. Powers “Asphalt Concrete Cracking Device to Evaluate Low Temperature Performance of HMA,” Journal of the Association of Asphalt Paving Technologists, Vol. 79, 2010, pp. 157-188.

20. U. Isacsso H. Zeng “Cracking of Asphalt at Low Temperature as Related to Bitumen Rheology,” Construction and Building Materials, 1998, pp. 83-91.

21. S. Kim “Direct Measurement of Asphalt Binder Thermal Cracking,” Journal of Materials in Civil Engineering, Vol, 17, No 6, 2005, pp. 632-639.

22. S. Kim, Z. Wysong and J. Kovach “Low Temperature Thermal Cracking of Asphalt Binder by Asphalt Binder Cracking Device,” In Transportation Research Record: Journal of the Transportation Research Board, No.1962, Transportation Research Board of the National Academies, Washington, D.C., 2006, pp. 28-35.

23. M. Marasteanu, X. Li, T.R. Clyne, V.R. Voller, D.H. Timm, D. E. and Newcomb “Low Temperature Cracking of Asphalt Concrete Pavements: Final Report,” Report No. MN/RC-2004-23, 2004, http://www.lrrb.org/PDF/200423.pdf, Accessed April 1st, 2010.

24. D. Jung and T.S. Vinson “Low Temperature Cracking Resistance of Asphalt Concrete Mixtures,” Journal of the Association of Asphalt Paving Technologists, Vol.62, 1993, pp. 54-87.

25. A. Epps “A Comparison of Measured and Predicted Low Temperature Cracking Conditions,” Journal of the Association of Asphalt Paving Technologists, Vol. 67, 1998, pg. 277-310.

26. M. Marasteanu, S. Dai, J.F. Labuz, X. and Li “Determining the Low Temperature Fracture Toughness of Asphalt Mixtures,” In Transportation Research Record: Journal of the Transportation Research Board, No.1789, Transportation Research Board of the National Academies, Washington, D.C., 2002, pp. 191-199.

27. W.G. Buttlar. And R. Roque "The Development of a Measurement and Analysis System to Accurately Determine Asphalt Concrete Properties Using the Indirect Tensile Mode," Journal of the Association of Asphalt Paving Technologists, Vol. 61, 1992, pg. 304-332.

28. W.G. Buttlar and R. Roque "Development and Evaluation of the Strategic Highway Research Program Measurement and Analysis System for Indirect Tensile Testing at Low Temperatures," In Transportation Research Record: Journal of the Transportation Research Board, No. 1454, Transportation Research Board of the National Academies, Washington, D.C., 1994, pg. 163-171.

29. Ramon Bonaquist "Refining the Simple Performance Tester for Use in Routine Practice" National Cooperative Highway Research Program (NCHRP), Report 614, 2008.

30. R. L. Lytton, J. Uzan, E. G. Fernando, R. Roque, D. Hiltumen, and S. M. Stoffels. "Development and Validation of Performance Prediction Models and Specifications for Asphalt Binders and Paving Mixes" National Research Council, Strategic Highway Research Program (SHRP) A-357, 1993.

31. S. Hu., X. Hu, F. Zhou, and L. Walubita. "SA-CrackPro: A New Finite Element Analysis Tool for Pavement Crack Propagation" Transportation Research Record, No. 2068, 2008.

32. "Tex-248-F: Overlay Test" Texas Department of Transportation, January 2009.

33. J.S. Daniel "Development of a Simplified Fatigue Test and Analysis Procedure using a Viscoelastic Continuum Damage Model and its Implementation to Westrack Mixture" Ph.D. Dissertation, North Carolina State University, Raleigh, NC, 2001.

34. G.R. Chehab "Characterization of Asphalt Concrete in Tension using a Viscoelastoplastic Model" PhD dissertation, North Carolina State University, Raleigh, NC, 2002.

35. R. Lundstromand U. Isacsson. "Asphalt Fatigue Modeling using Viscoelastic Continuum Damage Theory*"* Road Materials and Pavement Design, Vol. 4, No. 1, 2003.

36. M.E. Kutay, N.H. Gibson, J. Youtcheff, and R. Dongre. "Effect of Sample Size and Type on the Asphalt Fatigue Life Based on Viscoelastic Continuum Damage Theory" Transportation Research Record: Journal of the Transportation Research Board, 2009 (In Press).

37. Y.R. Kim and D.N. Little "One-dimensional Constitutive Modeling of Asphalt Concrete" ASCE Journal of Engineering Mechanics, Vol. 116, No. 4, 1990.

38. S. W. Park and R. A. Schapery, "Methods of Interconversion between Linear Viscoelastic Material Functions. Part I – a Numerical Method Based on Prony Series." International Journal of Solids and Structures, Vol. 36, 1999.